



Published in final edited form as:

J Immunol. 2020 November 01; 205(9): 2327–2341. doi:10.4049/jimmunol.1901430.

Focused ultrasound for immunomodulation of the tumor microenvironment

Jordan B. Joiner^a, Yuliya Pylayeva-Gupta^{b,c,*}, Paul A. Dayton^{a,c,d,*}

^aEshelman School of Pharmacy, University of North Carolina, Chapel Hill, NC 27599, USA

^bDepartment of Genetics, The Lineberger Comprehensive Cancer Center, University of North Carolina at Chapel Hill, Chapel Hill, NC 27599, USA

^cLineberger Comprehensive Cancer Center, University of North Carolina at Chapel Hill, Chapel Hill, NC 27599, USA

^dJoint Department of Biomedical Engineering, University of North Carolina and North Carolina State University, Chapel Hill, NC 27599, USA

Abstract

Focused ultrasound (FUS) has recently emerged as a modulator of the tumor microenvironment, paving the way for FUS to become a safe yet formidable cancer treatment option. Several mechanisms have been proposed for the role of FUS in facilitating immune responses and lowering drug delivery barriers. However, with the wide variety of FUS parameters used in diverse tumor types, it is challenging to pinpoint FUS specifications that may elicit the desired anti-tumor response. In order to clarify FUS bioeffects, we summarize four mechanisms of action, including thermal ablation, hyperthermia, mechanical perturbation, and histotripsy, each inducing unique vascular and immunological effects. Notable tumor responses to FUS include enhanced vascular permeability, increased T cell infiltration, and tumor growth suppression. Herein, we have categorized and reviewed recent methods of using therapeutic ultrasound to elicit an anti-tumor immune response with examples that reveal specific solutions and challenges in this new research area.

1. Introduction

A. Tumor microenvironment

The tumor microenvironment (TME) refers to normal tissue components around tumor cells, including extracellular matrix (ECM), stroma, blood and lymphatic vascular networks, and a variety of immune cell types (1, 2). These components work together to form harsh conditions that can promote tumor growth by limiting the function of normal immune cells. The TME can be broadly grouped into two classes: immunologically “cold” and “hot”. Cold, poorly immunogenic tumors, contain immune cells throughout the TME but lack cytotoxic

*Co-corresponding authors: Yuliya Pylayeva-Gupta: yuliyap1@email.unc.edu and Paul Dayton: padayton@email.unc.edu.

Competing Interests

P.A.D. declares he has equity interest in Triangle Biotechnology, Inc., as well as SonoVol, Inc., and is a co-inventor on licensed patents describing ultrasound imaging, therapy, and contrast agent technologies.

lymphocytes in the tumor core potentially due to defects in the tumor-associated vasculature or lack of priming and T cell recruitment (3). Immunologically hot TMEs have higher numbers of potential neoantigens and increased infiltration of cytotoxic lymphocytes.

Tumors are sites of chronic inflammation, fibrosis, angiogenesis, and essential cells that comprise the TME including immune cells, fibroblasts, vasculature, neuroendocrine cells and adipose cells (2). A multitude of mechanisms have been described, where cancer cells escape immune surveillance either by preventing antigen presentation and/or suppressing T cell activity (3). These include downregulation of major histocompatibility complex (MHC) levels on cancer cells, recruitment of regulatory cells including T_{regs}, myeloid-derived suppressor cells (MDSCs) and tumor-associated macrophages (TAMs) (4). Dysfunction of dendritic cells (DCs) contributes to poor T cell responses as CD4⁺ and CD8⁺ T cells can become anergic or self-inactivate due to the lack of co-stimulation (5). Cancer-associated fibroblasts form a tangled web of extracellular matrix fibers, which may block immune cells and drugs from entering the TME (6). In addition, neuroendocrine cells prevent cytotoxicity and migration of natural killer (NK) cells and cancer-associated adipose tissue establishes a pro-inflammatory environment (7,8). Together, cellular components of the TME contribute to an immunosuppressive environment and have been the target of several immunotherapies (9).

The TME is deeply intertwined with harsh biological and mechanical tumor properties, such as rigid stroma, high interstitial fluid pressure (IFP) and hypoxia. Matrix produced by cancer-associated fibroblasts contributes to the immunosuppressive environment by acting as a physical barrier to drugs and immune cells (10). High IFP is caused in part by stroma production and leaky vasculature (11). Compared to normal tissue pressure, which is typically around 0 mmHg, human tumor IFP can be anywhere from 10–40 mmHg depending on tumor type and stage (11–13). This drives interstitial flow within the tumor, promoting invasion of the lymphatic system, continuing the cycle of stroma stiffening and tumor progression (12). A major consequence of high IFP is synergy with lymphatic drainage, in which the tumor draining lymph node acts as a site for immune privilege and metastasis. Hypoxia, or limited tissue oxygenation, occurs due to the abnormal function and structure of blood vessels supplying the tumor and high oxygen consumption (15). Hypoxia causes tumor cells to release immunosuppressive molecules that suppress T-cell function, induce the differentiation of TAMs into M2 macrophages, suppress DC maturation and block receptors needed for cytotoxic NK cell activity (16). The components of the TME work together to protect tumor cells against the immune system, support tumor cell growth, facilitate metastasis, and contribute to a lack of efficacy of immunotherapy (17). Understanding the extent of tumor-specific immune surveillance and tumor heterogeneity can help predict responsiveness to immunotherapy, which is essential for improving upon and developing new approaches to cancer treatment.

B. Therapeutic Ultrasound

Therapeutic ultrasound has recently emerged as a modulator of the TME. Focused ultrasound (FUS) is typically performed using focused transducers that propagate mechanical waves focused to a small region, which results in high energy density absorbed

at the treatment spot (18). In contrast with diagnostic parameters, which utilize low energy to image a region without the introduction of bioeffects, therapeutic FUS is intended to generate biological effects such as tissue heating and mechanical stimulation, with potential for release of antigens and DAMPs that could stimulate immune responses (19–21). The combination of ultrasound parameters, type of tissue being treated, and the inclusion of microbubbles ultimately dictate the induced bioeffects. As summarized in Table 1, parameters that can be varied to generate bioeffects include frequency, pressure, duty cycle and treatment time. These parameters demonstrate significant overlap due to varying considerations including treatment depth, tissue type, presence of microbubbles and desired treatment effects. Frequency refers to the number of sound wave cycles emitted over a period of time, commonly measured in Hz (cycles per second). High frequency waves give high spatial resolution but lack penetration depth. Low frequency waves can penetrate deep into tissue with minimal attenuation. This is particularly important for clinical therapeutic ultrasound applications, such as treatment of uterine fibroids, in which mechanical waves penetrate 4–10 cm without damaging surrounding tissue (22). Ultrasound pressure, measured in Pascals, refers to the force emitted on a perpendicular surface area, and is equal to the amplitude of the sound wave. Ablative treatments require higher pressures, while non-ablative treatments use lower pressures (23). Duty cycle is equal to the percentage of time that ultrasound is on when operating in a pulsed on-and-off scheme. Because ultrasound attenuates rapidly in tissue to produce heat, thermal treatments use longer pulse lengths and non-thermal treatments require shorter, rapid pulsed treatments to avoid heating (24). The treatment time refers to the total amount of time it takes to scan the desired treatment area. The combination of these four parameters determines the total energy transmitted onto tissue. Because there is a large number of ultrasound parameter combinations that can generate both mechanical and thermal stresses, there is a continuum of bioeffects and immune responses that can be elicited. In order to better understand this, we have grouped four broad conceptual FUS treatment groups based on the type of stress induced: (1) thermal ablation, which causes coagulative tissue necrosis; (2) hyperthermia and thermal stress, which heats cells mildly without coagulation; (3) mechanical stimulation without thermal effects; and (4) histotripsy, which mechanically destroys tissue (Figure 1). The terms high-intensity focused ultrasound (HIFU), typically referring to destructive regimes such as thermal ablation and histotripsy, and low-intensity focused ultrasound (LOFU), typically referring to non-ablative thermal and mechanical effects, are commonly used when describing therapeutic ultrasound treatments. HIFU causes a high ratio of cell lysis to apoptosis and instantaneous cell death, while LOFU causes a high ratio of cell apoptosis to lysis, especially in short-pulsed treatments (25). It should be noted that HIFU and LOFU can elicit both thermal and mechanical effects and that the intensity range for each varies greatly on the application. The authors found ranges from 0.1–1000 W/cm² for LOFU and 35–10000 W/cm² for HIFU (26, 27).

Any FUS regime can be combined with intravenously administered microbubbles or phase change contrast agents (PCCA) to amplify and localize mechanical or thermal effects, allowing for the use of lower acoustic intensities and more accurate treatment localization in practice (Figure 2) (36–38). Microbubbles are gas-filled particles that oscillate rapidly and nonlinearly in response to acoustic waves, called cavitation (39,40). Although cavitation is a

complex phenomenon with a range of physical manifestations, scientists typically categorize microbubble cavitation into two regimes: stable and inertial. Stable cavitation exists when microbubbles gently and continuously oscillate as a response to FUS (41,42). This causes fluid convection called microstreaming, which generates moderate shear stress and increases intracellular Ca^{2+} concentration (43, 44). Inertial cavitation occurs when microbubbles expand and collapse violently, which generates high temperature and pressure within the bubble core, reactive oxygen species, and microjets that can permanently damage cells and tissue (45–47). When ultrasound waves come into contact with tissues, microbubbles, and cellular components, acoustic radiation force pushes oscillating microbubbles into vascular walls, increasing the quantity and magnitude of mechanical stress (48,49). In thermal regimes, bubbles or droplets can localize treatment and accelerate the rate of heating through shear flow at the bubble-tissue interface and energy generation at higher harmonic frequencies caused by bubble oscillation (50,51). In non-ablative regimes, microbubble oscillation can generate local shear which can modulate vasculature or disrupt cell membranes via sonoporation (52,53). The range of microbubble effects can be potentially utilized to achieve desired bioeffects and immune effects in combination with ultrasound parameters.

The bioeffects produced by each modality have been proposed to initiate release of stress signals, increase availability of antigens, and potentiate trafficking of dendritic cells, which may boost an immune response against the tumor (52). FUS can also affect aspects of tumor biology such as hypoxia, vascular permeability and interstitial fluid pressure (55,56). Responses to monotherapy FUS, however, tend to be transient and do not display robust systemic activation of anti-tumor immunity and/or T-cell memory (21,57). Recent advances in cancer immunotherapy have encouraged new studies to combine FUS with immunotherapy to produce systemic immune effects as shown in tables in this review. Surprisingly, few studies factor tumor-type intrinsic differences in TME, such as tumor cell cellularity and composition of stroma, in qualifying tumor FUS-responsiveness and determining the best course of treatment. Better understanding of how pre-treatment TME biology relates to efficacy may enable stratification and understanding of contributing mechanisms. For example, a recent study that compared FUS treatment with a range of pressures in two different models (B16F10 and 4T1) both demonstrated decreases in $\text{TGF-}\beta$ and IL-10 and increases in ICAM expression for both models, but differed in cytokine, chemokines and trophic factor (CCTF) expression between models (58). Combination of FUS treatments with immunotherapy, such as checkpoint blockade in pre-clinical models, has recently led to more durable abscopal immune responses, effect on metastasis and response to tumor re-challenges (59–62). Scenarios in which tumor burden is high may require the addition of systemic chemotherapy into immunotherapy-FUS treatment protocols (63). Linking specific parameters to immune outcomes is difficult at present due to inconsistent parameter reporting between groups and limited amount of studies in general. There are many more publications testing the immune effects of HIFU and thermal FUS than purely mechanical ultrasound treatments. In this review, we have categorized and summarized pre-clinical and clinical studies from the past 5 years using FUS therapy to elicit an immune response. These studies highlight advances in the field and consider the complex biological effects that FUS can provide to treat a variety of tumor types.

2. Thermal Ablation

Thermal ablation is the most utilized and characterized form of therapeutic ultrasound to date and the only FDA-approved form in cancer applications (64). Ultrasound in these regimes, typically referred to as HIFU, can be used as an alternative to surgery to noninvasively ablate tumors without damaging surrounding tissue (65). The transmission of sound waves at high pressure and duty cycle results in energy absorbed by the tissue at the focal spot that is converted to heat, resulting in rapid heating to temperatures of 60–85°C (65). This causes tissue coagulation and cell necrosis. Nearby tissue outside of the focal spot is heated to lower temperatures, causing cells to undergo thermal stress and eventually apoptosis (21). Cavitation of small bubbles in biological fluids and microbubbles or nanodroplets can be advantageous by providing focused and accelerated heating and additional mechanical damage (66,67). Passive cavitation detection (PCD) can be used to monitor cavitation effects and prevent unwanted mechanical damage to healthy tissue (68). Pre-clinical and clinical systems can produce lateral lesions in the millimeter size-range, allowing for precise treatment (69). Because tissue heating is dependent on ultrasound parameters, tissue density and local blood flow, image guidance and thermal monitoring is performed with ultrasound or magnetic resonance imaging (MRI) (70). Figure 3 depicts the relationship between ultrasound exposure time, temperature and tissue bioeffects. FDA-approved applications for HIFU include uterine fibroid ablation, essential tremor treatment, prostate tumor ablation and bone metastases pain treatment, paving the way for additional research in tumor treatment (71–74). Thermal ablation of tumors has the potential to be advantageous over conventional surgery and radiotherapy due to the precise treatment regime, lack of ionizing radiation, and obviation for incisional surgery, resulting in reduced complications due to infection and radiation-induced toxicity (75,76). HIFU is commonly an outpatient procedure, which can decrease patient time in the hospital compared to current surgical procedures (77). Due to the commonality of cancer recurrence and metastasis, a need to produce long-term anti-tumor effects, and the surge in cancer immunotherapy research, several clinical and preclinical studies which seek to understand the immune effect of tumor ablation have been published in recent years. Previously, the most common studies have used thermally ablated tumor debris as a vaccine, however HIFU alone has not yet proven sufficient to produce sufficient long-lasting systemic immunity.

A summary of the most recent studies using thermal ablation to modulate the tumor microenvironment is in Table 2. Thermal ablation causes specific cellular and vascular effects, including irreversible cell growth arrest, protein denaturation and reduced tumor blood flow due to endothelial cell swelling (78). Vascular effects of thermally ablated tumors have revealed occlusion of feeder vessels less than 2 mm in diameter, lack of vascular elasticity, disintegration of capillary endothelium and cavitation of peritubular cells (65). A large amount of tumor debris is generated, along with the release of damage-associated and heat-shock signals that can be sensed by local antigen presenting cells (21). It has been well-documented in early studies that HIFU ablation causes the release of heat shock proteins (HSPs), including HSP27, HSP60, HSP70, HSP72 and HSP73 which are taken up by antigen presenting cells, causing the activation of autologous cytotoxic T cells in both rodent models and humans (79–84). However, the modulation of downstream signal transduction

pathways in immune cell subsets as a result of HIFU treatments remains understudied (21). The ablation site also initiates wound-healing responses, attracting neutrophils, monocytes and macrophages to degrade necrotic tissue caused by ablation (85,86). Macrophages travel through the lymphatics to remove ablated tissue and may activate adaptive immune cells in the lymph node (87). Increase of mature dendritic cells and secretion of IFN- γ and IL-12 (88), as well as an increase in mature dendritic cell expression of MHC-II⁺, CD80⁺ and CD86⁺ has been demonstrated upon giving HIFU tumor debris as a vaccine (89). Antigens found in tumor debris, however, may be denatured depending upon ablation exposure, making them less immunogenic (90). Furthermore, the relative tumor vs. stromal tissue cellularity of the ablated site may dictate whether the ensuing immune response will result in priming or tolerance and should be considered when evaluating efficacy of responses. Whether the increase of wound healing immune cells in the ablated tumor region has a constructive or counteracting role in HIFU-mediated antitumor immune response remains to be studied. Infiltrating myeloid cells may be subject to tumor-mediated reprogramming into immunosuppressive tumor-associated macrophages and MDSC (91). There is an outstanding hypothesis that the rapid necrosis and localized coagulation caused by ablation minimizes time for danger-associated molecular pattern (DAMP) release compared to non-ablative regimes (92). This study compared thermal ablation with LOFU in treatment of B16F10 melanoma tumors, showing that in response to thermal ablation, populations of CD4⁺ and CD8⁺ cells remained constant and did not potentiate an increase in IL-2 from tumor lysates compared to LOFU (92). However, a different study demonstrated that combining thermal ablation with CpG immunostimulant in an ND1 tumor model produced an abscopal effect and recruited leukocytes, CD3⁺, CD4⁺, and CD8⁺ cells in contralateral tumors (59). Coincident ablation and immunotherapy diminished abscopal effects compared to dosing immunotherapy prior to FUS treatment, demonstrating the importance of timing when combining immunotherapy and HIFU (59). This study among others suggests that combining thermal ablation with immunotherapies such as CpG, anti-CD40 and anti-programmed cell death protein 1 (PD-1) can activate antigen presenting cells that are available to sense and process HIFU tumor debris (93). Furthermore, sparse-scan treatments that produce non-overlapping lesions have the potential to stimulate more potent immune effects (94). This study by Liu et al. found that the periphery of HIFU lesions had a higher number of infiltrating DCs, reserving more peripheral tumor tissue for DC stimulation and resulting in increased tumor growth suppression at tumor re-challenge (94). Although thermal ablation is a rapid method of removing and stopping progression of primary tumors, the resultant coagulative necrosis may dampen the release of immunostimulants within the TME which are needed to produce an adaptive response mediated by an increase in tumor-specific dendritic cells. For this reason, mass ablation alone at the tumor site as a vaccine currently seems to be insufficient to generate sustained antitumor immunity, especially for treating tumors prone to recurrence or metastasis. Treatments combining thermal ablation with immunotherapy appear to be a promising method for achieving systemic, long term effects. In summary, recent studies combining thermal ablation with immunotherapy have demonstrated recruitment and activation of MHC-II⁺ DCs, M1 macrophages, CD4⁺ and CD8⁺ T cells and NK cells, and a decrease in T_{reg} cells and MDSCs that have resulted in tumor growth suppression, decrease in tumor metastases, abscopal response in untreated tumors and complete response in pre-clinical models (21,59,60,92,95,96).

3. Thermal stress and hyperthermia

Focused ultrasound can also be used to heat tissue to mild temperatures (40–45°C) for seconds to a few minutes (thermal stress) or 30–90 minutes (hyperthermia) to induce specific bioeffects (97). Hyperthermia was first described over 5000 years ago in Egypt as a method of treating breast cancer with an instrument called the “fire drill” (98). Since then, this modality has been widely studied as a cancer therapy for its complex immune effects, thermally activated drug delivery and potential as a chemotherapy or radiotherapy adjuvant. Hyperthermia induced by a variety of methods causes protein and DNA damage and interferes with protein and DNA synthesis, disrupts cell cycle, and can result in direct cell death or apoptosis (99–101). As a result of these findings, extensive technologies including radiofrequency, microwaves, physical methods such as heated water and air, and focused ultrasound have been employed for inducing hyperthermia (102). Much of our understanding of known effects of hyperthermia stems from studies using more commonly used radiofrequency or microwave heating techniques, and while findings from these studies can be extrapolated, much is still unknown about specific cellular and vascular effects of ultrasound-induced heating. This is an important designation, because as compared to other hyperthermia techniques, ultrasound simultaneously induces mechanical effects (103). Several generations of ultrasound hyperthermia devices have been developed, including the Sonotherm 1000, the only FDA-approved ultrasound hyperthermia device, and the more recent Sonalleve system, the only commercially-available magnetic resonance imaging (MRgHIFU) device for hyperthermia applications (104). Despite the major advances in thermometry and treatment control, there is no FDA-approved cancer indication for ultrasound-induced heating, but clinical trials are ongoing for head and neck tumors, prostate and pelvic diseases and ovarian cancer.

There are several effects of hyperthermia that we can learn from non-ultrasound tissue heating techniques. The direct cytotoxic effects of hyperthermia include reversible growth arrest, which is realized by a brief decrease in RNA synthesis and prolonged decrease in DNA synthesis during the S and M phases (105). The lagging cell division causes some tumor cells to be killed via apoptosis (105). Hyperthermia also abrogates DNA repair mechanisms, which has been particularly useful in sensitization for radiation or chemotherapy treatment (106). Vasodilation is the main vascular effect of hyperthermia, leading to increased blood flow. This increased blood flow can mediate a reduction in hypoxia, acidosis and interstitial tumor pressure (103,107). Both innate and adaptive immune responses are triggered as a response to tissue heating, involving the activation of several types of immune cells (108). These effects are typically mediated by the release of DAMPs such as high mobility group box-1 (HMGB1) and lactate dehydrogenase (LDH) and cytokines such as interleukin (IL)-10, IL-6 and tumor necrosis factor α (TNF- α) (109). Heat shock proteins such as HSP70 are also expressed in response to stress in attempts to reverse protein misfolding and heat-induced cellular damage (110). Tissue heating has also been found to involve adaptive immunity, supported by the activation of cytotoxic T cells and induction of granzyme B, perforin and interferon γ (IFN γ) (111). Expression of intracellular adhesion molecules (ICAMs) also increases, leading to increased lymphocyte trafficking (112). Several of these effects have been tested in ultrasound hyperthermia applications,

especially with regards to cytokine and chemokine release and lymphocyte trafficking to tumors.

The effect of ultrasound-induced heating on cells is dependent on the temperature, length of exposure time and extent of cavitation (Figure 3) and can be generated by both HIFU, LOFU and unfocused ultrasound. Spontaneous cavitation that can occur at high pressures may cause mechanical damage and thermal necrosis, which has the potential to interfere with desired biological signaling processes (113,114). Multi-focal beams and feedback controls can be implemented to minimize cavitation and track temperature increase (115,116). Focused ultrasound treatments can take several hours due to the small focal point and can cause skin burns in shallow treatments, therefore non-focused treatments that can treat an entire tumor in one exposure may be advantageous for some tumor types (117–119). These non-focused ultrasound treatments have milder thermal and mechanical effects compared to HIFU. Short-term cell viability is retained in mild ultrasound-induced thermal treatments, with cell death progressing over a period of 2 to 48 hours after heat exposure (120). The use of high acoustic pressure is typically avoided in the case of thermal stress or hyperthermia because it causes extensive mechanical damage or thermal necrosis as in ablative regimes (118). However, some mechanical damage will still be caused using ultrasound, as evidenced by higher HSP70 expression in cells treated with HIFU than with temperature increase alone when heated to the same temperature for the same duration (121). Damage-associated effects caused by ultrasound such as these may lead to increased T cell recruitment. One of the first studies in 1994 monitoring the immune response of ultrasound-induced hyperthermia treatment in humans, demonstrated a normalization of CD4⁺/CD8⁺ T cell ratio in all patients one week after treatment of posterior choroidal melanoma tumors (122). Hyperthermia-inducing ultrasound treatments and immunological techniques have rapidly improved since this study, necessitating a review of more recent studies.

A summary of the most recent studies using FUS-induced thermal stress or hyperthermia to modulate the tumor microenvironment is in Table 3. Murine cell depletion studies have demonstrated that CD8⁺ T cells are the main effector cells, not CD4⁺ or NK cells, involved in an anti-CT26 tumor response using bubble liposomes and ultrasound to generate local thermal stress for 2 minutes (118). Tumor necrosis was evident at intensities higher than 3 W/cm² in combination with bubble liposomes, which corresponded with significant tumor volume decrease (118). Combination therapies with FUS-induced heating are also being explored, particularly in the field of thermoresponsive drug delivery vehicles. One study that combined heat-activatable doxorubicin, immunotherapy and FUS-induced hyperthermia for 25 minutes demonstrated a strong local and systemic immune effect in B16F10, NDL and MMTV-PyMT tumors (61). Significant tumoral CD8⁺ cell infiltration was observed for all mouse models, as well as complete tumor destruction in both treated and distant tumors (61). Notably, 90% of NDL mice treated with immunotherapy, heat-activated doxorubicin, and ultrasound were tumor free for 101 days (61). This study demonstrates a systemic effect of priming FUS-hyperthermia with immunotherapy dependent on dosing schedule, similar to thermal ablation. Another novel study combined ultrasound-induced hyperthermia with temperature-sensitive doxorubicin liposomes delivered by *Salmonella* “thermobots” for the immunomodulation of colon cancer (123). *In vivo* efficacy of C26 treatment with HIFU and thermobots for 30 minutes resulted in significant tumor regression compared to all other

groups over 5 days (123). The major immune mechanism finding in this study was increased polarization of macrophages to the pro-inflammatory M1 phenotype with HIFU and thermobot treatment (123). Shorter treatment times of 2 minutes can also induce necrosis and anti-tumor immune responses mediated by CD8⁺ cells when 3–4 W/cm² ultrasound is combined with microbubbles (118). Finally, another recent study utilized shorter ultrasound treatment times of 1.5 seconds per spot to heat prostate tumors to 45°C prior to radiotherapy to develop a T-cell driven in-situ tumor vaccine (124). While some preclinical and clinical studies can be found studying the anti-tumor effect of ultrasound-induced hyperthermia, more studies are needed to determine treatment parameters that will produce a specific immune response and whether these effects are superior to thermal ablation in certain cases. Treatments combining hyperthermia or thermal treatment with immunotherapy or chemotherapy appear to be a promising method for achieving systemic, long term effects. In summary, recent studies combining hyperthermia or thermal treatment with immunotherapy or chemotherapy have demonstrated recruitment and activation of MHC-II⁺ DCs, M1 macrophages, and CD4⁺ and CD8⁺ T cells (61,118,123). Some of these results have been correlated with reduced tumor growth, increased survival and abscopal response in untreated tumors in pre-clinical models; however, functional relevance was not demonstrated for CD4⁺ or NK cells in one study, implying that effects may be cancer type and context dependent (118).

4. Mechanical Perturbation

Ultrasound treatments that use low to moderate pressure and high duty cycle to mechanically disrupt cellular membranes and vascular endothelium without thermal effects are referred to here as mechanical perturbation. Parameters can be optimized for vasodilation and sonoporation, the temporary opening of cellular barriers including the blood-brain barrier (125,126). Microbubbles are commonly used to enhance mechanical effects through cavitation, or rapid expansion and contraction in response to acoustic pressure. Bioeffects of cavitation are highly dependent on whether bubbles are stably oscillating, which generates moderate shear stress, or violently breaking, which can cause cell death, damaged membranes, and altered cellular metabolism (127). The degree of cell membrane damage is directly related to the type of cell death that occurs; if the membrane can be repaired, the cell will either recover and survive or undergo apoptosis, and if the membrane cannot be repaired, the cell will undergo necrosis or lysis (128,129). Several studies have reported enhancement of drug delivery using LOFU and microbubbles (130). ARF is also generated on tissues, microbubbles, and cellular components, and is proportional to the differences in density and compressibility of objects in the acoustic field (47). ARF can push oscillating microbubbles in the direction of the primary acoustic field, which can be within the vasculature and into vascular walls, increasing the quantity and magnitude of mechanical stress (53).

A summary of the most recent studies using mechanical perturbation to modulate the tumor microenvironment is in Table 4. Although the observed anti-tumor responses have been stronger via mechanically-induced damage as compared with thermal effects, there is less information on the nature of immune mechanisms behind mechanically-induced tumor cell damage alone, which likely include a combination of time-dependent pro-inflammatory and

anti-inflammatory processes (131). Anti-inflammatory immune effects of LOFU have been explored in a data-mining study of cancer and non-cancer applications, demonstrating that mechanical effects transiently decreased inflammation and improved tissue repair by upregulating anti-inflammatory genes via B-cell translocation gene (TOB) in T cell signaling, G1/S checkpoint regulation, IL-10 signaling and the STAT3 pathway (132). LOFU also upregulated markers of MDSCs, MSCs, B1-B cells and T_{regs}, and induced exosome-mediated anti-inflammatory cytokines and miRNAs (132). While these responses may suppress anti-tumor immunity, the magnitude of these transient, in-vitro effects were not compared to pro-inflammatory effects or linked to changes in tumor growth (132). LOFU and microbubbles can decrease interstitial fluid pressure (IFP), which has been demonstrated in a study monitoring changes in tumor vascular properties caused by LOFU at varying pressures (56). Pressures of 5 MPa significantly decreased microvessel density, which in turn decreased IFP by 86.7%. Another study confirmed the necessity of microbubbles with mechanical-only treatments, resulting in a significant tumor volume decrease 16 days after treatment only after use with microbubbles (56). Flow cytometric analysis demonstrated a time-dependent response where CD4⁺Foxp3⁻ cells were significantly increased on day 1, but subsided after day 3, while CD8⁺ cells significantly increased on day 1 and continued to increase through day 18, demonstrating a transient immune effect (56).

Because non-ablative mechanical ultrasound has been shown to cause the release of DAMPs such as calreticulin and upregulate HSP70, MHC-II and B7 molecules indicating DC maturation, it is a promising adjuvant candidate for combination with radiotherapy, immunotherapy and chemotherapy to generate abscopal effects (92). A continuation of the study which compared LOFU with HIFU, as mentioned previously, explored the ability of LOFU to prevent T cell tolerance (92). Overall, LOFU alone was not enough to control tumor growth, but contributed to a complete response in 80% of immunocompetent mice and prevention of metastasis when combined with radiation (92). Lysates from LOFU-treated B16F10 melanoma tumor cells caused CD4⁺ T cells to produce significantly more IL-2 and to downregulate anergy-associated genes such as *Rnf123*, *Cblb*, *Itch* and *Egr2*. Hsp70 and MHC-I expression increased nearly 2-fold (92). Another study demonstrated that LOFU and microbubbles alone increased expression and localization of HSPs on 4T1 and TPSA23 cell surfaces (133). When this treatment was combined with radiotherapy, at least half of the TPSA23 mice were cured and were protected after tumor re-challenge (133). LOFU and microbubbles have also been combined with anti-PD-1 immunotherapy for the treatment of melanoma (92). Anti-PD-1 was dosed on the same day as ultrasound treatment and every three days until day 12 (92). Tumors that were treated with LOFU, microbubbles and anti-PD-1 were significantly smaller than all other groups at all timepoints and one mouse experienced complete tumor regression (92). This mouse also experienced complete tumor regression after a re-challenge with CT26 cells (92). However, there were no differences in counts of TILs between treatment groups and control, despite an increase of IFN- γ in tumor draining lymph nodes of treated mice (92). A significant amount of necrosis was observed by H&E stain, demonstrating that LOFU and microbubbles affected central regions of the tumor, while the anti-PD-1 acted upon the remainder of the tumor (92). This study highlights the potential for combining mechanical perturbation and immunotherapy; however, much is

still to be determined regarding the underlying mechanisms. Another study demonstrated that LOFU and microbubbles may be a promising chemosensitizer for solid tumors. Ultrasound and microbubbles alone induced cytoprotective pathways during UPR (unfolded protein response) and stem cell signaling pathways without resulting in cell death (134). The combination of this ultrasound treatment and 17AAG resulted in induction of cell apoptosis pathways of UPR, amplified ER (endoplasmic reticulum) stress and tumor growth regression in murine prostate tumors (134). Treatments combining low mechanical effects with immunotherapy appear to be a promising method for achieving systemic, long term effects. In summary, recent studies combining low mechanical effects with immunotherapy have demonstrated recruitment and activation of MHC-II⁺ DCs, CD4⁺ and CD8⁺ T cells and mast cells, and a decrease in anergy genes that have resulted in tumor growth suppression, increased survival, response to tumor re-challenge and potential for complete response in pre-clinical models (56,62,118,92).

5. Histotripsy

The fourth, and newest ultrasound regime used to elicit immune effects is histotripsy (also called M-HIFU), which uses extremely high pressure, short pulse ultrasound waves to mechanically fragment tissue into a liquefied homogenate that can be reabsorbed by the body (135,136). The traditional definition of histotripsy, also known as cavitation cloud histotripsy, refers to using microsecond-long waves to generate dense, cavitating bubble clouds which rapidly expand and contract (137) to mechanically break down tissue without significant thermal damage (138). These bubble clouds are formed when the peak negative pressure exceeds an intrinsic threshold, around 28 MPa for soft tissue (139), and can be generated either by using a single, negative pressure pulse (139) or by using multiple ultrasound pulses that form sparsely distributed bubbles that scatter positive shock fronts (137). Another form of histotripsy, called boiling histotripsy (BH), uses longer millisecond-long pulses to generate boiling bubbles that contact incident shockwaves to mechanically damage soft tissue (140). Boiling histotripsy can fractionate tissue into sub-cellular fragments either without thermal damage by using shorter pulses, or with thermal damage by using longer pulses (141). Clinical HIFU systems can perform boiling histotripsy protocols because lower peak pressures are required than in cavitation cloud histotripsy (142). The degree of mechanical damage induced by either type of histotripsy depends on the type of tissue, with more fibrotic tissue being more resistant to damage (143). Compared with thermal ablation, histotripsy also destroys tissue, but with a mechanically-dominated mechanism, which may result in the release of non-thermally damaged antigens (80,131). Boiling histotripsy has been compared with thermal ablation in a murine EL4 thymoma model (144). BH lesions revealed micro-hemorrhaging in a transition zone between disintegrated and vital tumor tissue, infiltration of granulocytes and macrophages 4 days after treatment, and densely packed dead and apoptotic cells, while thermally ablated lesions had no hemorrhaging, granulocytes and macrophages on the periphery of the lesion, and a core of heat-fixed cells (144). These results clearly show that BH and thermal ablation treatments have the potential for eliciting different immune responses. However, further studies are needed to understand the immune and vascular effects of histotripsy.

The first studies looking at immune effects of histotripsy showed dendritic cell infiltration to tumors and draining lymph nodes in a murine MC-38 model, metastatic tumor suppression in murine B16F10 tumors, and tumor growth inhibition, increase of CD8⁺ cells in spleens and draining lymph nodes and suppression of STAT3 activity in murine RM-9 tumors (131–148). These results indicate that complete tumor destruction using histotripsy can initiate an adaptive immune response. Studies using histotripsy to partially destroy tissue have led some authors to conclude that this treatment may increase the risk of metastasis due to increased vessel permeability and necrosis (149). However, a recent study that combines anti-CTLA-4 and anti-PD-L1 with sparse-scan histotripsy treatment of only 2% of murine neuroblastoma tumors demonstrated an increase in intratumoral CD4⁺ and CD8⁺ cells, dendritic cells in lymph nodes, and a significant abscopal effect with 61.1% survival of mice with untreated bilateral tumors (145). Based on these findings, it is important to consider the tumor type and vascularity when designing histotripsy protocols to maximize tumor blood supply and immune sensitization. Finally, a recent study comparing histotripsy with unfractionated ablative radiation and thermal ablation in subcutaneous B16F10 melanoma tumors demonstrated significantly higher intertumoral CD8⁺ infiltration in histotripsy-treated tumors (146). Furthermore, histotripsy-treated tumors were able to upregulate intertumoral NK, DC, neutrophil, B and T cell populations, circulating NK cells and tumor antigen GP33 specific CD8⁺ cells, and translocation of calreticulin and HMGB1, demonstrating local and systemic inflammatory responses (146). While few preliminary studies have shown that histotripsy can activate the adaptive immune system, there is a need for additional published studies to understand immune cells involved in multiple tumor types with a variety of histotripsy treatment schemes. So far, studies have demonstrated that histotripsy can recruit dendritic cells, granulocytes, macrophages, NK cells, CD4⁺ and CD8⁺ T cells and downregulate STAT3 signaling in immune cells (131–148).

6. Future Directions

Mechanistic understanding for combinational applications

While each ultrasound regime has the capability of initiating an immune response, it is still unknown which regimes have the greatest anti-tumor biological effect on each tumor type and which FUS regimes synergize best with combinatorial approaches. Because of the relatively few studies, expansive combinations of ultrasound parameter inputs, lack of thorough input reporting and variety of immune markers to be explored, additional reproducible studies are needed to understand how to best utilize ultrasound to treat tumors. A common theme is that the long-term immune effect of non-ablative FUS regimes has the potential to be greater than ablative treatments due to limited tissue necrosis and cell death caused by non-ablative treatments, increasing time for antigen release and processing. However, mechanical perturbation treatments in combination with immunotherapy have yet to be published. For tumors that are easily accessible and less prone to metastasis, thermal ablation may be beneficial. For late stage, immunosuppressive tumors that are prone to metastasis, a more aggressive and combinatorial treatment such as non-ablative heating or mechanical perturbation and immunotherapy, radiotherapy, or chemotherapy may be beneficial for long-term antitumor immunity. Ultrasound alone has not been proven to elicit long-term response, therefore multiple treatments and/or combinatorial treatments are

needed to enhance the response, as evidenced by examples from the studies described in this review.

Because each tumor type and stage of disease has vastly different immune microenvironment features, vascular composition and metastatic tendencies, future preclinical studies on FUS-immunology should focus on comparing ultrasound treatments and combination therapies to determine the best course of action for one tumor type and at different growth stages. Immunomodulatory agents aimed at activating antigen presenting cells, such as CpG and anti-CD40, or checkpoint-blockade therapies such as anti-PD1 or CTLA-4 should be considered for both pre-clinical and clinical trials because of the evidenced involvement of dendritic cells and T cells upon ultrasound treatment (150–152). Further optimization of ultrasound parameters and treatment timing is needed to translate these treatments to clinic.

Clinical translation

Currently, therapeutic ultrasound is FDA approved for the treatment of bone metastases, essential tremors, tremor-dominated Parkinson's Disease, prostate cancer, benign prostatic hyperplasia, and uterine fibroids, with research in progress for 126 separate indications. The first clinical trial combining focused ultrasound with an immunotherapy drug began in 2017 ([NCT03237572](#)) for the treatment of metastatic or unresectable breast cancer. The study will evaluate the effect of dosing pembrolizumab (anti-PD-1) before or after HIFU thermal ablation of 50% of the tumor. The primary outcome will assess a change in CD8⁺/CD4⁺ T cell ratio in the ablation zone and the secondary outcome will assess adverse events. Clearly, the effects caused by thermal ablation are thought to be T cell dependent. A recent human trial demonstrated significant therapeutic benefit in addition to increased levels of NK, CD3⁺, CD4⁺, CD8⁺ cells three months after thermal ablation of liver tumors (153). Another clinical trial that combined FUS-hyperthermia and thermally sensitive drug-loaded particles, although lacking immune endpoints, demonstrated clinical translation of therapeutic ultrasound for cancer treatments (154). Using ultrasound to increase vascular permeability, interstitial fluid flow and perfusion could address the large disparity of nanoparticle success in the clinic by aiding in solid tumor penetration (155,156). Immune effects and endpoints need further clarification in order to design the most optimal dosing regimen for FUS combination with immunotherapy.

7. Conclusions

Preclinical and clinical trials have demonstrated the use of FUS as an immunomodulatory cancer treatment. Bioeffects are highly dependent on ultrasound parameters used, frequency of treatment, combinatorial treatments, and tumor model utilized. Although grouping ultrasound treatments is helpful for understanding the vast array of FUS physical effects, immune effects overlap between groups, and inconsistent parameter reporting prevents linking specific parameters to immune effects. While different ultrasound treatments are varying in their physical effects and extent of cell damage, these appear to overall result in similar immune cell filtration types without a clear indication of which ultrasound treatment is superior to another in treating a single tumor type. Generally, ablative ultrasound regimes

cause immunogenic cell death and generate tumor debris, but alone lack sufficient antigen presentation for consistent anti-tumor immunity (133). In comparison, non-ablative ultrasound regimes release stress signals more slowly to attract antigen presenting cells, but the lack of immunogenic cell death and immune cell priming results in a transient response. Understanding the short-term and long-term immune and vascular effects of each ultrasound treatment group is vital for clinical translation, especially if the cancer type is prone to metastasis or if a sustained abscopal effect is desired. For all ultrasound treatments, regardless of group, the combination with immunotherapy is required to create a sustained and systemic immune response. The recruitment of healthy immune cells, particularly macrophages, dendritic cells and CD8⁺ T cells is linked to an anti-tumor immune response that can boost abscopal effects and improve anti-tumor effects of chemotherapy, immunotherapy and radiotherapy. However, limited primary literature and mechanistic understanding of how ultrasound potentiates these responses for various tumor models currently prevents clinical translation. Specific limitations include how and when stress signals are produced by tumor cells and the role of FUS in tumor immunosuppression, cellular signaling transduction pathways, metastasis, T cell anergy and abscopal effects. It is unknown whether tumor cells can become resistant to FUS treatment. The use of different FUS systems and inconsistent parameter reporting makes understanding and repeating studies difficult. For continued advancement, it is imperative for authors to report critical parameters including frequency, pressure, duty cycle and treatment time. More studies on FUS bioeffects and immune effects are needed in order to rationally design FUS treatments for the long-term treatment of cancer.

Acknowledgments

Grants support information

The authors wish to acknowledge support from the National Science Foundation Graduate Research Fellowship Program (J.B.J.), National Institutes of Health (R21 CA246550 (P.A.D. and Y. P.-G.)) and R37 CA230786 (Y.P.-G.), University Cancer Research Fund, UNC Lineberger Comprehensive Cancer Center and North Carolina Translational and Clinical Sciences Institute, NC Tracs (TTSA023P1) for research support.

References

1. Chen F, Zhuang X, Lin L, Yu P, Wang Y, Shi Y, Hu G & Sun Y 2015 New horizons in tumor microenvironment biology: challenges and opportunities. *BMC Med.*13:45. [PubMed: 25857315]
2. Binnewies M, Roberts EW, Kersten K, Chan V, Fearon DF, Merad M, Coussens LM, Gabrilovich DI, Ostrand-Rosenberg S, Hedrick CC, Vonderheide RH, Pittet MJ, Jain RK, Zou W, Howcroft TK, Woodhouse EC, Weinberg RA, & Krummel MF. 2018 Understanding the tumor immune microenvironment (TIME) for effective therapy. *Nat Med.* 5;24(5):541–550. doi: 10.1038/s41591-018-0014-x. [PubMed: 29686425]
3. Bonaventura P, Shekarian T, Alcazer V, Valladeau-Guilemond J, Valsesia-Wittmann S, Amigorena S, Caux C & Depil S 2019 Cold Tumors: A Therapeutic Challenge for Immunotherapy. *Front. Immunol* 10:168. doi: 10.3389/fimmu.2019.00168 [PubMed: 30800125]
4. Wang M, Zhao J, Zhang L, Wei F, Lian Y, Wu Y, Gong Z, Zhang S, Zhou J, Cao K, Li X, Xiong W, Li G, Zeng Z & Guo C. 2017. Role of tumor microenvironment in tumorigenesis. *J Cancer.* 2017;8(5):761–773. doi:10.7150/jca.17648 [PubMed: 28382138]
5. Sotomayor EM, Borrello I, Rattis FM, Cuenca AG, Abrams J, Staveley-O'Carroll K & Levitsky H. 2001 Cross-presentation of tumor antigens by bone marrow-derived antigen-presenting cells is the dominant mechanism in the induction of T-cell tolerance during B-cell lymphoma progression. *Blood.* 98:1070–7. doi: 10.1182/blood.V98.4.1070 [PubMed: 11493453]

6. Liu T, Zhou L, Li D, Andl T, Zhang Y. 2019 Cancer-Associated Fibroblasts Build and Secure the Tumor Microenvironment. *Front Cell Dev Biol.* 4 24;7:60. doi: 10.3389/fcell.2019.00060. [PubMed: 31106200]
7. Lang K, Drell TL, Niggemann B, Zanker KS, and Entschladen F. 2003 Neurotransmitters regulate the migration and cytotoxicity in natural killer cells. *Immunol Lett.* 90:165–72. [PubMed: 14687720]
8. Tilg H and Moschen AR. 2006 Adipocytokines: mediators linking adipose tissue, inflammation and immunity. *Nat Rev Immunol.* 6 (10) pp. 772–783 [PubMed: 16998510]
9. Sharma P, Hu-Lieskovan S, Wargo JA, & Ribas A 2017 Primary, Adaptive, and Acquired Resistance to Cancer Immunotherapy. *Cell.* 168(4), 707–723. 10.1016/j.cell.2017.01.017 [PubMed: 28187290]
10. Elahi-Gedwillo KY, Carlson M, Zettervall J, & Provenzano PP 2019 Antifibrotic Therapy Disrupts Stromal Barriers and Modulates the Immune Landscape in Pancreatic Ductal Adenocarcinoma. *Cancer Research.* 79(2), 372 LP–386. 10.1158/0008-5472.CAN-18-1334 [PubMed: 30401713]
11. Heldin CH, Rubin K, Pietras K & Ostman, 2004 A. High interstitial fluid pressure - an obstacle in cancer therapy. *Nature Rev. Cancer* 4, 806–813. [PubMed: 15510161]
12. Less JR, Posner MC, Boucher Y, Borochovit D, Wolmark N, Jain RK. 1992 Interstitial hypertension in human breast and colorectal tumors. *Cancer Res.* 52(22):6371–6374. [PubMed: 1423283]
13. Boucher Y, Kirkwood JM, Opacic D, Desantis M, Jain RK. 1991 Interstitial hypertension in superficial metastatic melanomas in humans. *Cancer Res.* 51(24):6691–6694. [PubMed: 1742743]
14. Provenzano PP, Inman DR, Eliceiri KW, Knittel JG, Yan L, Rueden CT, White JG, Keely PJ. 2008 Collagen density promotes mammary tumor initiation and progression. *BMC Med.* 6:11. doi: 10.1186/1741-7015-6-11. [PubMed: 18442412]
15. Rofstad EK, Galappathi K, & Mathiesen BS 2014 Tumor Interstitial Fluid Pressure—A Link between Tumor Hypoxia, Microvascular Density, and Lymph Node Metastasis. *Neoplasia.* 16(7), 586–594. 10.1016/j.neo.2014.07.003 [PubMed: 25117980]
16. Barsoum IB, Koti M, Siemens DR, & Graham CH 2014 Mechanisms of Hypoxia-Mediated Immune Escape in Cancer. *Cancer Research.* 74(24), 7185 LP–7190. 10.1158/0008-5472.CAN-14-2598 [PubMed: 25344227]
17. Sambhi M, Bagheri L, & Szewczuk MR 2019 Current Challenges in Cancer Immunotherapy: Multimodal Approaches to Improve Efficacy and Patient Response Rates. *Journal of Oncology.* 4508794 10.1155/2019/4508794
18. Ter Haar G, Sinnott D, & Rivens I 1989 High intensity focused ultrasound—a surgical technique for the treatment of discrete liver tumours. *Physics in Medicine and Biology.* 34(11), 1743–1750. 10.1088/0031-9155/34/11/021 [PubMed: 2685839]
19. Miller DL, Smith NB, Bailey MR, Czarnota GJ, Hynynen K, Makin IR. 2012 Overview of therapeutic ultrasound applications and safety considerations. *J Ultrasound Med.* 4;31(4):623–34. doi: 10.7863/jum.2012.31.4.623. [PubMed: 22441920]
20. Hynynen K, & Jolesz FA 1998 Demonstration of Potential Noninvasive Ultrasound Brain Therapy Through an Intact Skull. *Ultrasound in Medicine & Biology.* 24(2), 275–283. [PubMed: 9550186]
21. van den Bijgaart RJE, Eikelenboom DC, Hoogenboom M, Fütterer JJ, den Brok MH, & Adema GJ 2017 Thermal and mechanical high-intensity focused ultrasound: perspectives on tumor ablation, immune effects and combination strategies. *Cancer Immunology, Immunotherapy.* 66(2), 247–258. 10.1007/s00262-016-1891-9 [PubMed: 27585790]
22. Zhao W-P, Chen J-Y, Zhang L, Li Q, Qin J, Peng S, Li K-Q, Wang Z-B, & Chen W-Z 2013 Feasibility of ultrasound-guided high intensity focused ultrasound ablating uterine fibroids with hyperintense on T2-weighted MR imaging. *European Journal of Radiology.* 82(1), e43–e49. 10.1016/j.ejrad.2012.08.020 [PubMed: 23000188]
23. Mauri G, Nicosia L, Xu Z, Di Pietro S, Monfardini L, Bonomo G, Varano GM, Prada F, Della Vigna P, Orsi F. 2018 Focused ultrasound: tumour ablation and its potential to enhance immunological therapy to cancer. *Br J Radiol.* 91(1083):20170641. doi: 10.1259/bjr.20170641. [PubMed: 29168922]
24. Fang HY, Tsai KC, Cheng WH, Shieh MJ, Lou PJ, Lin WL & Chen WS. 2007 The effects of power on–off durations of pulsed ultrasound on the destruction of cancer cells. *International*

- Journal of Hyperthermia, 23:4, 371–380, DOI: 10.1080/02656730701342409 [PubMed: 17558736]
25. Shi G, Zhong M, Ye F, Zhang X. 2019 Low-frequency HIFU induced cancer immunotherapy: tempting challenges and potential opportunities. *Cancer Biol Med.* 16(4):714–728. doi: 10.20892/j.issn.2095-3941.2019.0232. [PubMed: 31908890]
 26. Rosenschein U, Furman V, Kerner E, Fabian I, & Bernheim J 2000 Ultrasound Imaging – Guided Noninvasive Ultrasound Thrombolysis. *Circulation.* 238–245. 10.1161/01.CIR.102.2.238 [PubMed: 10889137]
 27. Copelan A, Hartman J, Chehab M, Venkatesan AM. 2015 High-Intensity Focused Ultrasound: Current Status for Image-Guided Therapy. *Semin Intervent Radiol.* 32(4):398–415. doi: 10.1055/s-0035-1564793. [PubMed: 26622104]
 28. Bove T, Zawada T, Serup J, Jessen A, Poli M 2019 High-frequency (20-MHz) high-intensity focused ultrasound (HIFU) system for dermal intervention: Preclinical evaluation in skin equivalents. *Skin Res Technol.* 25: 217–228. 10.1111/srt.12661 [PubMed: 30620418]
 29. Zhao L-Y, Zou J-Z, Chen Z-G, Liu S, Jiao J, & Wu F 2016 Acoustic Cavitation Enhances Focused Ultrasound Ablation with Phase-Shift Inorganic Perfluorohexane Nanoemulsions: An In Vitro Study Using a Clinical Device. *BioMed Research International.* 7936902 10.1155/2016/7936902
 30. Zhou YF. 2011 High intensity focused ultrasound in clinical tumor ablation. *World J Clin Oncol.* 2(1):8–27. doi: 10.5306/wjco.v2.i1.8. [PubMed: 21603311]
 31. Wan M, Feng Y, & Haar G. ter. 2015 *Cavitation in Biomedicine Principles and Techniques.* Dordrecht: Springer Netherlands.
 32. Guillemin PC, Gui L, Lorton O, Zilli T, Crowe LA, Desgranges S, Montet X, Terraz S, Miralbell R, Salomir R & Boudabbous S 2019 Mild hyperthermia by MR-guided focused ultrasound in an ex vivo model of osteolytic bone tumour: optimization of the spatio-temporal control of the delivered temperature. *J Transl Med* 17, 350 10.1186/s12967-019-2094-x [PubMed: 31651311]
 33. Speed CA, 2001 Therapeutic ultrasound in soft tissue lesions, *Rheumatology*, 40;12:1331–1336, 10.1093/rheumatology/40.12.1331 [PubMed: 11752501]
 34. Izadifar Z, Babyn P, & Chapman D 2017 Mechanical and Biological Effects of Ultrasound: A Review of Present Knowledge. *Ultrasound in Medicine and Biology*, 43(6), 1085–1104. 10.1016/j.ultrasmedbio.2017.01.023 [PubMed: 28342566]
 35. Riesberg G, Bigelow TA, Stessman DJ, Spalding MH, Yao L, Wang T, & Xu J (2014). Flow rate and duty cycle effects in lysis of *Chlamydomonas reinhardtii* using high-energy pulsed focused ultrasound. *The Journal of the Acoustical Society of America*, 135(6), 3632–3638. 10.1121/1.4874627 [PubMed: 24916410]
 36. Holt RG, & Roy RA 2001 Measurements of bubble-enhanced heating from focused, mhz-frequency ultrasound in a tissue-mimicking material. *Ultrasound in Medicine & Biology*, 27(10), 1399–1412. [PubMed: 11731053]
 37. Moyer LC, Timbie KF, Sheeran PS, Price RJ, Miller GW, Dayton PA. 2015 High-intensity focused ultrasound ablation enhancement in vivo via phase-shift nanodroplets compared to microbubbles. *J Ther Ultrasound.* 5 27;3:7. doi: 10.1186/s40349-015-0029-4. [PubMed: 26045964]
 38. Tung YS, Liu HL, Wu CC, Ju KC, Chen WS, Lin WL. 2006 Contrast-agent-enhanced ultrasound thermal ablation. *Ultrasound Med Biol.* 32(7):1103–1110. doi:10.1016/j.ultrasmedbio.2006.04.005 [PubMed: 16829324]
 39. Lauterborn W, & Kurz T 2010 Physics of bubble oscillations. *Reports on Progress in Physics.* 73(10), 106501 10.1088/0034-4885/73/10/106501
 40. Flynn HG. 1959 Physics of acoustic cavitation. *J Acoust Soc Am* 31: 1582.
 41. Bader KB, & Holland CK 2013 Gauging the likelihood of stable cavitation from ultrasound contrast agents. *Physics in Medicine and Biology*, 58(1), 127–144. 10.1088/0031-9155/58/1/127 [PubMed: 23221109]
 42. Margulis MA 1993 *Sonochemistry and Cavitation*; Gordon Breach Science Publishers: Langhorne, PA, USA.
 43. Fan P, Zhang Y, Guo X, Cai C, Wang M, Yang D, Li Y, Tu J, Crum LA, Wu J, Zhang D. 2017 Cell-cycle-specific Cellular Responses to Sonoporation. *Theranostics* 2017; 7(19):4894–4908. doi:10.7150/thno.20820. [PubMed: 29187912]

44. Fan Z, Kumon RE, Park J, Deng CX. 2010 Intracellular delivery and calcium transients generated in sonoporation facilitated by microbubbles. *J Control Release*. 142(1):31–39. [PubMed: 19818371]
45. Wu J, Nyborg WL. 2008 Ultrasound, cavitation bubbles and their interaction with cells. *Adv Drug Deliv Rev*. 60:1103–16. doi: 10.1016/j.addr.2008.03.009. [PubMed: 18468716]
46. Riesz P, & Kondo T 1992 Free radical formation induced by ultrasound and its biological implications. *Free Radical Biology and Medicine*, 13(3), 247–270. [PubMed: 1324205]
47. Fan P, Zhang Y, Guo X, Cai C, Wang M, Yang D, Li Y, Tu J, Crum LA, Wu J, Zhang D. Cell-cycle-specific Cellular Responses to Sonoporation. *Theranostics*. 2017 11 3;7(19):4894–4908. doi: 10.7150/thno.20820. [PubMed: 29187912]
48. Caskey CF, Qin S, Dayton PA, Ferrara KW. 2009 Microbubble tunneling in gel phantoms. *J Acoust Soc Am*. 125(5):EL183–9. doi: 10.1121/1.3097679. [PubMed: 19425620]
49. Yemane PT, Åslund AKO, Snipstad S, Bjørkøy A, Grendstad K, Berg S, Mørch Y, Torp S, Hansen R, Davies C. de L. 2019 Effect of Ultrasound on the Vasculature and Extravasation of Nanoscale Particles Imaged in Real Time. *Ultrasound in Medicine & Biology*, 45(11), 3028–3041. 10.1016/j.ultrasmedbio.2019.07.683 [PubMed: 31474384]
50. O'Brien WD. Ultrasound-biophysics mechanisms. 2007 *Prog Biophys Mol Biol*. 93:212–55. doi: 10.1016/j.pbiomolbio.2006.07.010. [PubMed: 16934858]
51. Moyer LC, Timbie KF, Sheeran PS, Price RJ, Miller GW, Dayton PA. 2015 High-intensity focused ultrasound ablation enhancement in vivo via phase-shift nanodroplets compared to microbubbles. *J Ther Ultrasound*. 3:7. doi: 10.1186/s40349-015-0029-4. [PubMed: 26045964]
52. Beekers I, Vegter M, Lattwein KR, Mastik F, Beurskens R, van der Steen AFW, de Jong N, Verweij MD, Kooiman K 2020 Opening of endothelial cell–cell contacts due to sonoporation. *Journal of Controlled Release*, 322(1), 426–438. 10.1016/j.jconrel.2020.03.038 [PubMed: 32246975]
53. Gao Z, Zheng J, Yang B, Wang Z, Fan H, Lv Y, Li H, Jia L, Cao W 2013 Sonodynamic therapy inhibits angiogenesis and tumor growth in a xenograft mouse model. *Cancer Letters*, 335(1), 93–99. 10.1016/j.canlet.2013.02.006 [PubMed: 23402818]
54. Xu W, Zhang X, Hu X, Zhiyi C, & Huang P 2019 Translational Prospects of ultrasound-mediated tumor immunotherapy: Preclinical advances and safety considerations. *Cancer Letters*, 460, 86–95. 10.1016/j.canlet.2019.06.017 [PubMed: 31254552]
55. Hou R, Xu Y, Lu Q, Zhang Y, & Hu B 2017 Effect of low-frequency low-intensity ultrasound with microbubbles on prostate cancer hypoxia. *Tumor Biology*, 39(10), 1–9. 10.1177/1010428317719275
56. Zhang Q, Jin H, Chen L, Chen Q, He Y, Yang Y, Ma S, Xiao S, Xi F, Luo Q and Liu J. 2019 Effect of Ultrasound Combined With Microbubble Therapy on Interstitial Fluid Pressure and VX2 Tumor Structure in Rabbit. *Front. Pharmacol*. 10:716. doi: 10.3389/fphar.2019.00716 [PubMed: 31293427]
57. Liu HL, Hsieh HY, Lu LA, Kang CW, Wu MF, Lin CY. 2012 Low-pressure pulsed focused ultrasound with microbubbles promotes an anticancer immunological response. *J Transl Med*. 2012;10:221. doi:10.1186/1479-5876-10-221 [PubMed: 23140567]
58. Aydin O, Chandran P, Lorsung RR, Cohen G, Burks SR, & Frank JA 2019 The Proteomic Effects of Pulsed Focused Ultrasound on Tumor Microenvironments of Murine Melanoma and Breast Cancer Models. *Ultrasound in Medicine & Biology*, 45(12), 3232–3245. 10.1016/j.ultrasmedbio.2019.08.014 [PubMed: 31530419]
59. Silvestrini MT, Ingham ES, Mahakian LM, Kheiroloom A, Liu Y, Fite BZ, Tam SM, Tucci ST, Watson KT, Wong AW, Monjazebe AM, Hubbard NE, Murphy WJ, Borowsky AD & Ferrara KW 2017 Priming is key to effective incorporation of image-guided thermal ablation into immunotherapy protocols. *JCI Insight*, 2(6). 10.1172/jci.insight.90521
60. Chavez M, Silvestrini MT, Ingham ES, Fite BZ, Mahakian LM, Tam SM, Ilovitsh A, Monjazebe AM, Murphy WJ, Hubbard NE, Davis RR, Tepper CG, Borowsky AD, Ferrara KW. 2018 Distinct immune signatures in directly treated and distant tumors result from TLR adjuvants and focal ablation. *Theranostics* 8(13):3611–3628. doi:10.7150/thno.25613. [PubMed: 30026870]
61. Kheiroloom A, Silvestrini MT, Ingham ES, Mahakian LM, Tam SM, Tumbale SK, Foiret J, Hubbard N, Borowsky W & Ferrara KW 2019 Combining activatable nanodelivery with

- immunotherapy in a murine breast cancer model. *Journal of Controlled Release*, 303, 42–54. 10.1016/j.jconrel.2019.04.008 [PubMed: 30978432]
62. Bulner S, Prodeus A, Garipey J, Hynynen K & Goertz D 2019 “Enhancing Checkpoint Inhibitor Therapy with Ultrasound Stimulated Microbubbles” *Ultrasound in Medicine and Biology*, Volume 45, Issue 2, 500–51. [PubMed: 30447880]
 63. Monjazebe AM, Hsiao HH, Sckisel GD, & Murphy WJ 2012 The role of antigen-specific and non-specific immunotherapy in the treatment of cancer. *Journal of Immunotoxicology*, 9(3), 248–258. 10.3109/1547691X.2012.685527 [PubMed: 22734880]
 64. Elhelf IAS, Albahar H, Shah U, Oto A, Cressman E, & Almekkawy M 2018 High intensity focused ultrasound: The fundamentals, clinical applications and research trends. *Diagnostic and Interventional Imaging*, 99(6), 349–359. 10.1016/j.diii.2018.03.001 [PubMed: 29778401]
 65. Guan L, Xu G 2016 Damage effect of high-intensity focused ultrasound on breast cancer tissues and their vascularities. *World J Surg Onc*. 14, 153 10.1186/s12957-016-0908-3
 66. Hynynen K, Chung A, Colucci V, Jolesz F. 1996 Potential adverse effects of high-intensity focused ultrasound exposure on blood vessels in vivo. *Ultrasound Med Biol*. 22(2):193–201. [PubMed: 8735529]
 67. Taguchi K, Takagi R, Yasuda J, Yoshizawa S, & Umemura S 2016 Study on cavitation behavior during high-intensity focused ultrasound exposure by using optical and ultrasonic imaging. *Japanese Journal of Applied Physics*, 55(7S1), 07KF22 10.7567/jjap.55.07kf22
 68. McLaughlan J, Rivens I, Leighton T, ter Haar G. 2010 A study of bubble activity generated in ex-vivo tissue by HIFU. *Ultrasound Med Biol*. 36(8):1327–44. [PubMed: 20691922]
 69. Xiao-Ying Zhang, Hua Duan, Jin-Juan Wang, Ying-Shu Guo, Jiu-Mei Cheng, Hong Ye & Zang Chun-Yi. 2019 Clinical analysis of high-intensity focused ultrasound ablation for abdominal wall endometriosis: a 4-year experience at a specialty gynecological institution. *International Journal of Hyperthermia*, 36:1, 87–94, DOI: 10.1080/02656736.2018.1534276 [PubMed: 30428731]
 70. McDannold Nathan et al. Preclinical evaluation of a low-frequency transcranial MRI-guided focused ultrasound system in a primate model. 2016 *Phys. Med. Biol* 61 7664 DOI: 10.1088/0031-9155/61/21/7664 [PubMed: 27740941]
 71. Hesley GK, Gorny KR, Henrichsen TL, Woodrum DA & Brown DL 2008 A Clinical Review of Focused Ultrasound Ablation With Magnetic Resonance Guidance: An Option for Treating Uterine Fibroid. *Ultrasound Quarterly*, 24(2), 131–139. doi: 10.1097/RUQ.0b013e31817c5e0c. [PubMed: 18528271]
 72. Rohani M, & Fasano A 2017 Focused Ultrasound for Essential Tremor: Review of the Evidence and Discussion of Current Hurdles. *Tremor and other hyperkinetic movements*. 7, 462 10.7916/D8Z89JN1
 73. Chaussy CG, & Thüroff S 2017 High-Intensity Focused Ultrasound for the Treatment of Prostate Cancer: A Review. *Journal of Endourology*, 31(S1), S-30–S-37. 10.1089/end.2016.0548 [PubMed: 28355119]
 74. Bertrand AS, Iannessi A, Natale R, Beaumont H, Patriti S, Xiong-Ying J, Baudin G, & Thyss A 2018 Focused ultrasound for the treatment of bone metastases: effectiveness and feasibility. *Journal of therapeutic ultrasound*, 6, 8 10.1186/s40349-018-0117-3 [PubMed: 30519467]
 75. Yang R, Reilly CR, Rescorla FJ, Sanghvi NT, Fry FJ, Franklin TD, & Grosfeld JL 1992 Effects of high-intensity focused ultrasound in the treatment of experimental neuroblastoma. *Journal of Pediatric Surgery*, 27(2), 246–251. 10.1016/0022-3468(92)90321-W [PubMed: 1564625]
 76. Alkhorayef M, Mahmoud MZ, Alzimami KS, Sulieman A, Fagiri MA. High-Intensity Focused Ultrasound (HIFU) in Localized Prostate Cancer Treatment. 2015 *Pol J Radiol*. 80:131–41. doi: 10.12659/PJR.892341. [PubMed: 25806099]
 77. Yu SCH, Cheung ECW, Leung VYF, & Fung LWY 2019 Oxytocin-Augmented and Non-Sedating High-Intensity-Focused Ultrasound (HIFU) for Uterine Fibroids Showed Promising Outcome As Compared To HIFU Alone or Uterine Artery Embolization. *Ultrasound in Medicine and Biology*, 45(12), 3207–3213. 10.1016/j.ultrasmedbio.2019.07.410 [PubMed: 31493956]
 78. Rampersaud EN, Vujaskovic Z, and Inman BA. 2010 “Hyperthermia as a treatment for bladder cancer,” *Oncology*. 24;12:1149–1155 [PubMed: 21141697]

79. Wu F, Wang ZB, Cao YD, Zhou Q, Zhang Y, Zhu XQ. 2007 Expression of tumor antigens and heat shock protein 70 in breast cancer cells after high intensity focused ultrasound ablation. *Ann Surg Oncol.* 14, 1237–1242. [PubMed: 17187168]
80. Hu Z, Yang XY, Liu Y, Morse MA, Lyster HK, Clay TM, Zhong P. 2005 Release of endogenous danger signals from HIFU-treated tumor cells and their stimulatory effects on APCs. *Biochem Biophys Res Commun.* 335:124–131. [PubMed: 16055092]
81. Madersbacher S, Grobl M, Kramer G, Dirnhofner S, Steiner GE, Marberger M. 1998 Regulation of heat shock protein 27 expression of prostatic cells in response to heat treatment. *Prostate.* 37:174–181. [PubMed: 9792134]
82. Kramer G, Steiner GE, Grobl M, Hrachowitz K, Reithmayr F, Paucz L, Newman M, Madersbacher S, Gruber D, Susani M, Marberger M. 2004 Response to sublethal heat treatment of prostatic tumor cells and of prostatic tumor infiltrating T-cells. *Prostate* 58:109–120. [PubMed: 14716736]
83. Xia JZ, Xie FL, Ran LF, Xie XP, Fan YM, & Wu F 2012 High-Intensity Focused Ultrasound Tumor Ablation Activates Autologous Tumor-Specific Cytotoxic T Lymphocytes. *Ultrasound in Medicine and Biology.* 38(8), 1363–1371. 10.1016/j.ultrasmedbio.2012.03.009 [PubMed: 22633269]
84. Wu F, Wang Z-B, Lu P, Xu Z-L, Chen W-Z, Zhu H, & Jin C-B 2004 Activated anti-tumor immunity in cancer patients after high intensity focused ultrasound ablation. *Ultrasound in Medicine & Biology.* 30(9), 1217–1222. 10.1016/j.ultrasmedbio.2004.08.003 [PubMed: 15550325]
85. Xie B, Li YY, Jia L, Nie YQ, Du H, & Jiang SM 2010 Experimental ablation of the pancreas with high intensity focused ultrasound (HIFU) in a porcine model. *International Journal of Medical Sciences.* 8(1), 9–15. 10.7150/ijms.8.9 [PubMed: 21197259]
86. Fatemi A 2009 High-Intensity Focused Ultrasound Effectively Reduces Adipose Tissue. *Seminars in Cutaneous Medicine and Surgery.* THE WOODLANDS: FRONTLINE MEDICAL COMMUNICATIONS. 10.1016/j.sder.2009.11.005
87. Liao S and von der Weid PY. 2015 Lymphatic system: an active pathway for immune protection. *Semin Cell Dev Biol.* 38:83–9. doi: 10.1016/j.semcdb.2014.11.012. [PubMed: 25534659]
88. Deng J, Zhang Y, Feng J & Wu F 2010 Dendritic Cells Loaded with Ultrasound-Ablated Tumour Induce in vivo Specific Antitumour Immune Responses. *Ultrasound in Medicine & Biology.* 36;3:441–448. 10.1016/j.ultrasmedbio.2009.12.004. [PubMed: 20172447]
89. Zhang Y, Deng J, Feng J, Wu F. 2010 Enhancement of antitumor vaccine in ablated hepatocellular carcinoma by high-intensity focused ultrasound. *World J Gastroenterol.* 16(28):3584–3591. doi:10.3748/wjg.v16.i28.3584 [PubMed: 20653069]
90. Koch C, Jensen SS, Øster A and Houen G 1996 A comparison of the immunogenicity of the native and denatured forms of a protein. *APMIS.* 104: 115–125. doi:10.1111/j.1699-0463.1996.tb00696.x [PubMed: 8619913]
91. Fleming V, Hu X, Weber R, Nagibin V, Groth C, Altevogt P, Utikal J, Umansky V. 2018 Targeting Myeloid-Derived Suppressor Cells to Bypass Tumor-Induced Immunosuppression. *Front Immunol.* 9:398. doi: 10.3389/fimmu.2018.00398. [PubMed: 29552012]
92. Bandyopadhyay S, Quinn TJ, Scanduzzi L, Basu I, Partanen A, Tomé WA, Macian F, Guha C. 2016 Low-Intensity Focused Ultrasound Induces Reversal of Tumor-Induced T Cell Tolerance and Prevents Immune Escape. *J Immunol.* 196(4):1964–76. doi: 10.4049/jimmunol.1500541. [PubMed: 26755821]
93. Singh MP, Sethuraman SN, Ritchey J, Fiering S, Guha C, Malayer J, & Ranjan A 2019 In-situ vaccination using focused ultrasound heating and anti-CD-40 agonistic antibody enhances T-cell mediated local and abscopal effects in murine melanoma. *International Journal of Hyperthermia.* 36(Sup1), 64–73. 10.1080/02656736.2019.1663280
94. Liu F, Hu Z, Qiu L, Hui C, Li C, Zhong P, & Zhang J 2010 Boosting high-intensity focused ultrasound-induced anti-tumor immunity using a sparse-scan strategy that can more effectively promote dendritic cell maturation. *Journal of Translational Medicine.* 8, 1–12. 10.1186/1479-5876-8-7 [PubMed: 20064266]
95. Yuan S, Li H, Yang M, Zha H, Sun H, Li X, Li A, Gu Y, Duan L, Luo J, Li C, Wang Y, Wang Z, He T, Zhou L 2015 High intensity focused ultrasound enhances anti-tumor immunity by inhibiting

- the negative regulatory effect of miR-134 on CD86 in a murine melanoma model. *Oncotarget*. 6: 37626–37637 [PubMed: 26485753]
96. Ran Li-Feng, Xie Xun-Peng, Xia Ji-Zhu, Xie Fang-Lin, Fan Yan-Min & Wu Feng. 2016 Specific antitumour immunity of HIFU-activated cytotoxic T lymphocytes after adoptive transfusion in tumour-bearing mice. *International Journal of Hyperthermia*. 32:2, 204–210, DOI: 10.3109/02656736.2015.1112438 [PubMed: 26708472]
 97. Diederich CJ, & Hynynen K 1999 Ultrasound technology for hyperthermia. *Ultrasound in Medicine & Biology*. 25(6), 871–887. 10.1016/S0301-5629(99)00048-4 [PubMed: 10461714]
 98. Breasted JH. 1930 *The Edwin Smith surgical papyrus*. Chicago: University of Chicago Oriental Institute Publications.
 99. Engin K 1996 Biological rationale and clinical experience with hyperthermia. *Control Clin Trials*. 17:316–42. [PubMed: 8889346]
 100. Lepock JR. 2004 Role of nuclear protein denaturation and aggregation in thermal radiosensitization. *Int J Hyperthermia*. 20:115–30. [PubMed: 15195506]
 101. Roti Roti JL. 2008 Cellular responses to hyperthermia (40–46 degrees C): cell killing and molecular events. *Int J Hyperthermia*. 24:3–15. [PubMed: 18214765]
 102. Bredlau AL, McCrackin MA, Motamarry A, Helke K, Chen C, Broome AM, Haemmerich D. *Thermal Therapy Approaches for Treatment of Brain Tumors in Animals and Humans*. 2016 *Crit Rev Biomed Eng*. 44(6):443–457. doi: 10.1615/CritRevBiomedEng.2017021249. [PubMed: 29431091]
 103. Elming PB; Sørensen BS; Oei AL; Franken NA; Crezee J; Overgaard J; Horsman MR 2019 Hyperthermia: The Optimal Treatment to Overcome Radiation Resistant Hypoxia. *Cancers*. 11, 60.
 104. Zhu L, Altman MB, Laszlo A, Straube W, Zoberi I, Hallahan DE, & Chen H 2019 Ultrasound Hyperthermia Technology for Radiosensitization. *Ultrasound in medicine & biology*, 45(5), 1025–1043. 10.1016/j.ultrasmedbio.2018.12.007 [PubMed: 30773377]
 105. Hildebrandt B, Wust P, Ahlers O, Dieing A, Sreenivasa G, Kerner T, Felix R & Riess H 2002 The cellular and molecular basis of hyperthermia. *Critical Reviews in Oncology/Hematology*, 43(1), 33–56. 10.1016/S1040-8428(01)00179-2. [PubMed: 12098606]
 106. Oei AL, Vriend LE, Crezee J, Franken NA, Krawczyk PM. 2015 Effects of hyperthermia on DNA repair pathways: one treatment to inhibit them all. *Radiat Oncol*. 10:165. doi:10.1186/s13014-015-0462-0 [PubMed: 26245485]
 107. Winslow TB, Eranki A, Ullas S, Singh AK, Repasky EA, Sen A. 2015 A pilot study of the effects of mild systemic heating on human head and neck tumour xenografts: Analysis of tumour perfusion, interstitial fluid pressure, hypoxia and efficacy of radiation therapy. *Int J Hyperthermia*. 31(6):693–701. doi: 10.3109/02656736.2015.1037800. [PubMed: 25986432]
 108. Baronzio GF, Seta RD, D'Amico M, Baronzio A, Freitas I, Forzenigo G, Gramaglia A, Hager ED. 2009 Effects of Local and Whole Body Hyperthermia on Immunity In: *Madame Curie Bioscience Database* [Internet]. Austin (TX): Landes Bioscience; 2000–2013. Available from: <https://www.ncbi.nlm.nih.gov/books/NBK6083/>
 109. Chen T, Guo J, Han C, Yang M, & Cao X 2009 Heat Shock Protein 70, Released from Heat-Stressed Tumor Cells, Initiates Antitumor Immunity by Inducing Tumor Cell Chemokine Production and Activating Dendritic Cells via TLR4 Pathway. *The Journal of Immunology*, 182(3), 1449 LP–1459. 10.4049/jimmunol.182.3.1449 [PubMed: 19155492]
 110. Singh IS; Hasday JD 2013 Fever, hyperthermia and the heat shock response. *Int. J. Hyperth*. 29, 423–435.
 111. Takahashi A; Torigoe T; Tamura Y; Kanaseki T; Tsukahara T; Sasaki Y; Kameshima H; Tsuruma T; Hirata K; Tokino T; Hirohashi Y & Sato N 2012 Heat shock enhances the expression of cytotoxic granule proteins and augments the activities of tumor-associated antigen-specific cytotoxic T lymphocytes. *Cell Stress Chaperones*. 17, 757–763. [PubMed: 22777894]
 112. Chen Q, Appenheimer MM, Muhitch JB, Fisher DT, Clancy KA, Miecznikowski JC, Wang WC, Evans SS. 2009 Thermal facilitation of lymphocyte trafficking involves temporal induction of intravascular ICAM-1. *Microcirculation*. 16(2):143–158. doi: 10.1080/10739680802353850. [PubMed: 19031292]

113. Hynynen K, Chung AH, Colucci V, & Jolesz FA 1996 Potential adverse effects of high-intensity focused ultrasound exposure on blood vessels in vivo. *Ultrasound in Medicine & Biology*, 22(2), 193–201. 10.1016/0301-5629(95)02044-6 [PubMed: 8735529]
114. Mochizuki H, & Hattori N 2018 MR-Guided Focused Ultrasound. *Brain and Nerve*. 70(2), 147–153. 10.11477/mf.1416200967 [PubMed: 29433116]
115. Chaplin V, & Caskey CF 2017 Multi-focal HIFU reduces cavitation in mild-hyperthermia. *Journal of therapeutic ultrasound*, 5, 12 10.1186/s40349-017-0089-8 [PubMed: 28413682]
116. Desjoux C, Poizat A, Gilles B, Inserra C, & Bera J-C 2013 Control of inertial acoustic cavitation in pulsed sonication using a real-time feedback loop system. *The Journal of the Acoustical Society of America*, 134(2), 1640–1646. 10.1121/1.4812973 [PubMed: 23927204]
117. Coon J, Todd N, & Roemer R 2012 HIFU treatment time reduction through heating approach optimisation. *International Journal of Hyperthermia*, 28(8), 799–820. 10.3109/02656736.2012.738846 [PubMed: 23153221]
118. Suzuki R, Oda Y, Omata D, Nishiie N, Koshima R, Shiono Y, Sawaguchi Y, Unga J, Naoi T, Kawakami S, Hashida M & Maruyama K 2016 Tumor growth suppression by the combination of nanobubbles and ultrasound. *Cancer Science*, 107(3), 217–223. 10.1111/cas.12867 [PubMed: 26707839]
119. Li JJ, Xu GL, Gu MF, Luo GY, Rong Z, Wu PH, Xia JC. 2007 Complications of high intensity focused ultrasound in patients with recurrent and metastatic abdominal tumors. *World J Gastroenterol*. 13(19):2747–51. doi: 10.3748/wjg.v13.i19.2747. [PubMed: 17569147]
120. Marmor JB, Hilerio FJ, Hahn GM. 1979 Tumor eradication and cell survival after localized hyperthermia induced by ultrasound. *Cancer Res*. 39(6 Pt 1):2166–2171. [PubMed: 445414]
121. Hundt W, O’Connell-Rodwell CE, Bednarski MD, Steinbach S, & Guccione S 2007. In Vitro Effect of Focused Ultrasound or Thermal Stress on HSP70 Expression and Cell Viability in Three Tumor Cell Lines. *Academic Radiology*, 14(7), 859–870. 10.1016/j.acra.2007.04.008 [PubMed: 17574136]
122. Rosberger DF, Coleman DJ, Silverman R, Woods S, Rondeau M, and Cunningham-Rundles S. 1994 “Immunomodulation in choroidal melanoma: reversal of inverted CD4/CD8 ratios following treatment with ultrasonic hyperthermia.,” *Biotechnol. Ther* 5; 1–2:59–68 [PubMed: 7703833]
123. Ektate K, Munteanu MC, Ashar H, Malayer J, & Ranjan A 2018 Chemo-immunotherapy of colon cancer with focused ultrasound and Salmonella-laden temperature sensitive liposomes (thermobots). *Scientific Reports*, 8(1), 13062 10.1038/s41598-018-30106-4 [PubMed: 30166607]
124. Skalina KA, Singh S, Chavez CG, Macian F & Guha C 2019 Low Intensity Focused Ultrasound (LOFU)-mediated Acoustic Immune Priming and Ablative Radiation Therapy for in situ Tumor Vaccines. *Sci Rep* 9, 15516 10.1038/s41598-019-51332-4 [PubMed: 31664044]
125. Abrahao A, Meng Y, Llinas M, Huang Y, Hamani C, Mainprize T, Aubert I, Heyn C, Black SE, Hynynen K, Lipsman N, Zinman L. 2019 First-in-human trial of blood-brain barrier opening in amyotrophic lateral sclerosis using MR-guided focused ultrasound. *Nat Commun*. 10(1):4373. doi: 10.1038/s41467-019-12426-9. [PubMed: 31558719]
126. Le Floc’h J, Lu HD, Lim TL, Démoré C, Prud’homme RK, Hynynen K, & Foster FS 2019 Transcranial Photoacoustic Detection of Blood-Brain Barrier Disruption Following Focused Ultrasound-Mediated Nanoparticle Delivery. *Molecular Imaging and Biology*. 10.1007/s11307-019-01397-4
127. Wörle K; Steinbach P; Hofstädter F 1994 The Combined Effects of High-Energy Shock Waves and Cytostatic Drugs or Cytokines on Human Bladder Cancer Cells. *Br. J. Cancer*. 69, 58–65. [PubMed: 8286211]
128. Lejbkowitz F, Salzberg S. 1997 Distinct sensitivity of normal and malignant cells to ultrasound in vitro. *Environ Health Perspect*. 105:1575–8. [PubMed: 9467085]
129. Feril LB Jr, Kondo T. 2004 Biological effects of low intensity ultrasound: the mechanism involved, and its implications on therapy and on biosafety of ultrasound. *J Radiat Res*. 45:479–89. doi: 10.1269/jrr.45.479. [PubMed: 15635256]

130. Mullin LB, Phillips LC, Dayton PA. 2013 Nanoparticle delivery enhancement with acoustically activated microbubbles. *IEEE Trans Ultrason Ferroelectr Freq Control*. 60(1):65–77. doi: 10.1109/TUFFC.2013.2538. [PubMed: 23287914]
131. Hu Z, Yang XY, Liu Y, Sankin GN, Pua EC, Morse MA, Lyerly HK, Clay TM, & Zhong P 2007 Investigation of HIFU-induced anti-tumor immunity in a murine tumor model. *J Transl Med*. 11:5–34.
132. Yang Q, Nanayakkara GK, Drummer C, Sun Y, Johnson C, Cueto R, Fu H, Shao Y, Wang L, Yang WY, Tang P, Liu L-W, Ge S, Zhou X-D, Khan M, Want H, & Yang X 2017 Low-Intensity Ultrasound-Induced Anti-inflammatory Effects Are Mediated by Several New Mechanisms Including Gene Induction, Immunosuppressor Cell Promotion, and Enhancement of Exosome Biogenesis and Docking. *Frontiers in Physiology*. 8:818 Doi: 10.3389/fphys.2017.00818. [PubMed: 29109687]
133. Skalina KA, Singh S, Chavez CG, Macian F, & Guha C 2019 Low Intensity Focused Ultrasound (LOFU)-mediated Acoustic Immune Priming and Ablative Radiation Therapy for in situ Tumor Vaccines. *Scientific Reports*, 9(1), 1–12. 10.1038/s41598-019-51332-4 [PubMed: 30626917]
134. Saha S, Bhanja P, Partanen A, Zhang W, Liu L, Tomé WA, & Guha C 2014 Low intensity focused ultrasound (LOFU) modulates cancer response and sensitizes prostate cancer to 17AAG. *Oncoscience*, 1(6), 434–445. 10.18632/oncoscience.48 [PubMed: 25594042]
135. Vlaisavljevich E, Greve J, Cheng X, Ives K, Shi J, Jin L, Arvidson A, Hall T, Welling TH, Owens G, Roberts W, Xu Z. 2016 Non-Invasive Ultrasound Liver Ablation Using Histotripsy: Chronic Study in an In Vivo Rodent Model. *Ultrasound Med Biol*. 42(8):1890–902. doi: 10.1016/j.ultrasmedbio.2016.03.018. [PubMed: 27140521]
136. Bader KB, Vlaisavljevich E, & Maxwell AD 2019 For Whom the Bubble Grows: Physical Principles of Bubble Nucleation and Dynamics in Histotripsy Ultrasound Therapy. *Ultrasound in Medicine & Biology*, 45(5), 1056–1080. [PubMed: 30922619]
137. Maxwell AD, Wang TY, Cain CA, Fowlkes JB, Sapozhnikov OA, Bailey MR, Xu Z. (2011) Cavitation clouds created by shock scattering from bubbles during histotripsy. *J Acoust Soc Am*. 130(4):1888–98. doi: 10.1121/1.3625239. [PubMed: 21973343]
138. Lundt JE, Allen SP, Shi J, Hall TL, Cain CA, & Xu Z 2017 Non-invasive, Rapid Ablation of Tissue Volume Using Histotripsy. *Ultrasound in Medicine & Biology*, 43(12), 2834–2847. [PubMed: 28935135]
139. Lin K, Kim Y, Maxwell AD, Wang T, Hall TL, Xu Z, Fowlkes JB, & Cain CA 2014 Histotripsy beyond the intrinsic cavitation threshold using very short ultrasound pulses: microtripsy. *IEEE Transactions on Ultrasonics, Ferroelectrics, and Frequency Control*, 61(2), 251–265.
140. Khokhlova VA, Fowlkes JB, Roberts WW, Schade GR, Xu Z, Khokhlova TD, Hall TL, Maxwell AD, Wang YN, Cain CA. 2015 Histotripsy methods in mechanical disintegration of tissue: towards clinical applications. *Int J Hyperthermia*. 31(2):145–62. doi: 10.3109/02656736.2015.1007538. [PubMed: 25707817]
141. Wang YN, Khokhlova T, Bailey M, Hwang JH, Khokhlova V. 2013 Histological and biochemical analysis of mechanical and thermal bioeffects in boiling histotripsy lesions induced by high intensity focused ultrasound. *Ultrasound Med Biol*. 39(3):424–438. doi:10.1016/j.ultrasmedbio.2012.10.012 [PubMed: 23312958]
142. Eranki A, Farr N, Partanen A, V Sharma K, Chen H, Rossi CT, Kothapalli SV, Oetgen M, Kim A, H Negussie A, Woods D, J Wood B, C W Kim P, S Yarmolenko P. 2017 Boiling histotripsy lesion characterization on a clinical magnetic resonance imaging-guided high intensity focused ultrasound system. *PLoS One*. 12(3):e0173867. doi: 10.1371/journal.pone.0173867. [PubMed: 28301597]
143. Vlaisavljevich E, Kim Y, Owens G, Roberts W, Cain C, Xu Z. 2014 Effects of tissue mechanical properties on susceptibility to histotripsy-induced tissue damage. *Phys Med Biol*. 59(2):253–270. doi:10.1088/0031-9155/59/2/253 [PubMed: 24351722]
144. Hoogenboom M, Eikelenboom D, den Brok MH, Veltien A, Wassink M, Wesseling P, Dumont E, Futterer JJ, Adema GJ & Heerschap A 2016 In vivo MR guided boiling histotripsy in a mouse tumor model evaluated by MRI and histopathology. *NMR in Biomedicine*. 29(6), 721–731. 10.1002/nbm.3520 [PubMed: 27061290]

145. Eranki A, Srinivasan P, Ries M, Kim A, Lazarski CA, Rossi CT, Khokhlova TD, Wilson E, Knoblach SM, Sharma KV, Wood BJ, Moonen C, Sandler AD & Kim PCW 2019 High Intensity Focused Ultrasound (HIFU) Triggers Immune Sensitization of Refractory Murine Neuroblastoma to Checkpoint Inhibitor Therapy. *Clinical Cancer Research*. 26:1152–61. 10.1158/1078-0432.ccr-19-1604 [PubMed: 31615935]
146. Qu S, Worlikar T, Felsted AE, Ganguly A, Beems MV, Hubbard R, Pepple AL, Kevelin AA, Garavaglia H, Dib J, Toma M, Huang H, Tsung A, Xu Z, & Cho CS 2020 Non-thermal histotripsy tumor ablation promotes abscopal immune responses that enhance cancer immunotherapy. *Journal for ImmunoTherapy of Cancer*. 8(1), 1–12. 10.1136/jitc-2019-000200
147. Xing Y, Lu X, Pua EC, Zhong P. 2008 The effect of high intensity focused ultrasound treatment on metastases in a murine melanoma model. *Biochem Biophys Res Commun*. 375(4):645–650. [PubMed: 18727919]
148. Huang X, Yuan F, Liang M, Lo HW, Shinohara ML, Robertson C & Zhong P 2012 M-HIFU inhibits tumor growth, suppresses STAT3 activity and enhances tumor specific immunity in a transplant tumor model of prostate cancer. *PLoS One*. 7(7):e41632. [PubMed: 22911830]
149. Hancock H, Dreher MR, Crawford N, Pollock CB, Shih J, Wood BJ, Hunter K & Frenkel V 2009 *Clin Exp Metastasis*. 26: 729 10.1007/s10585-009-9272-9 [PubMed: 19517258]
150. Nierkens S, den Brok MH, Roelofsen T, Wagenaars JA, Figdor CG, Ruers TJ, Adema GJ. 2009 Route of administration of the TLR9 agonist CpG critically determines the efficacy of cancer immunotherapy in mice. *PLoS ONE* 4:e8368. [PubMed: 20020049]
151. Nierkens S, den Brok MH, Garcia Z, Togher S, Wagenaars J, Wassink M, Boon L, Ruers TJ, Figdor CG, Schoenberger SP, Adema GJ, Janssen EM. 2011 Immune adjuvant efficacy of CpG oligonucleotide in cancer treatment is founded specifically upon TLR9 function in plasmacytoid dendritic cells. *Cancer Res*. 71:6428–6437. [PubMed: 21788345]
152. Waitz R, Solomon SB, Petre EN, Trumble AE, Fasso M, Norton L, Allison JP. 2012 Potent induction of tumor immunity by combining tumor cryoablation with anti-CTLA-4 therapy. *Cancer Res*. 72:430–439. [PubMed: 22108823]
153. Ma B, Liu X, Yu Z. 2019 The Effect of High Intensity Focused Ultrasound on the Treatment of Liver Cancer and Patients' Immunity. *Cancer Biomarkers* 24; 1: 85–90. DOI: 10.3233/CBM-181822 [PubMed: 30347603]
154. Tak WY, Lin S-M, Wang Y, Zheng J, Vecchione A, Park SY, Chen M, Wong S, Xu R, Peng C, Chiou Y, Huang G, Cai J, Abdullah B, Lee J, Lee J, Choi J, Gopez-Cervantes J, Sherman M, Finn R, Omata M, O'Neal M, Makris L, Borys N, Poon R & Lencioni R 2018 Phase III HEAT Study Adding Lyso-Thermosensitive Liposomal Doxorubicin to Radiofrequency Ablation in Patients with Unresectable Hepatocellular Carcinoma Lesions. *Clinical Cancer Research*, 24(1), 73 LP–83. 10.1158/1078-0432.CCR-16-2433 [PubMed: 29018051]
155. Pan Y, Yoon S, Sun J, Huang Z, Lee C, Allen M, Wu Y, Chang Y, Sadlain M, Shung K, Chien S & Wang Y 2018 Mechanogenetics for the remote and noninvasive control of cancer immunotherapy. *Proceedings of the National Academy of Sciences*, 115(5), 992 LP–997. 10.1073/pnas.1714900115
156. Li L, ten Hagen TLM, Bolkestein M, Gasselhuber A, Yatvin J, van Rhooen GC, Eggermont A, Haemmerich D & Koning GA 2013 Improved intratumoral nanoparticle extravasation and penetration by mild hyperthermia. *Journal of Controlled Release*, 167(2), 130–137. [PubMed: 23391444]
157. Pozzi S 2015 High Intensity Focused Ultrasound (HIFU): computing tools for medical applications. 10.13140/RG.2.1.5098.2166

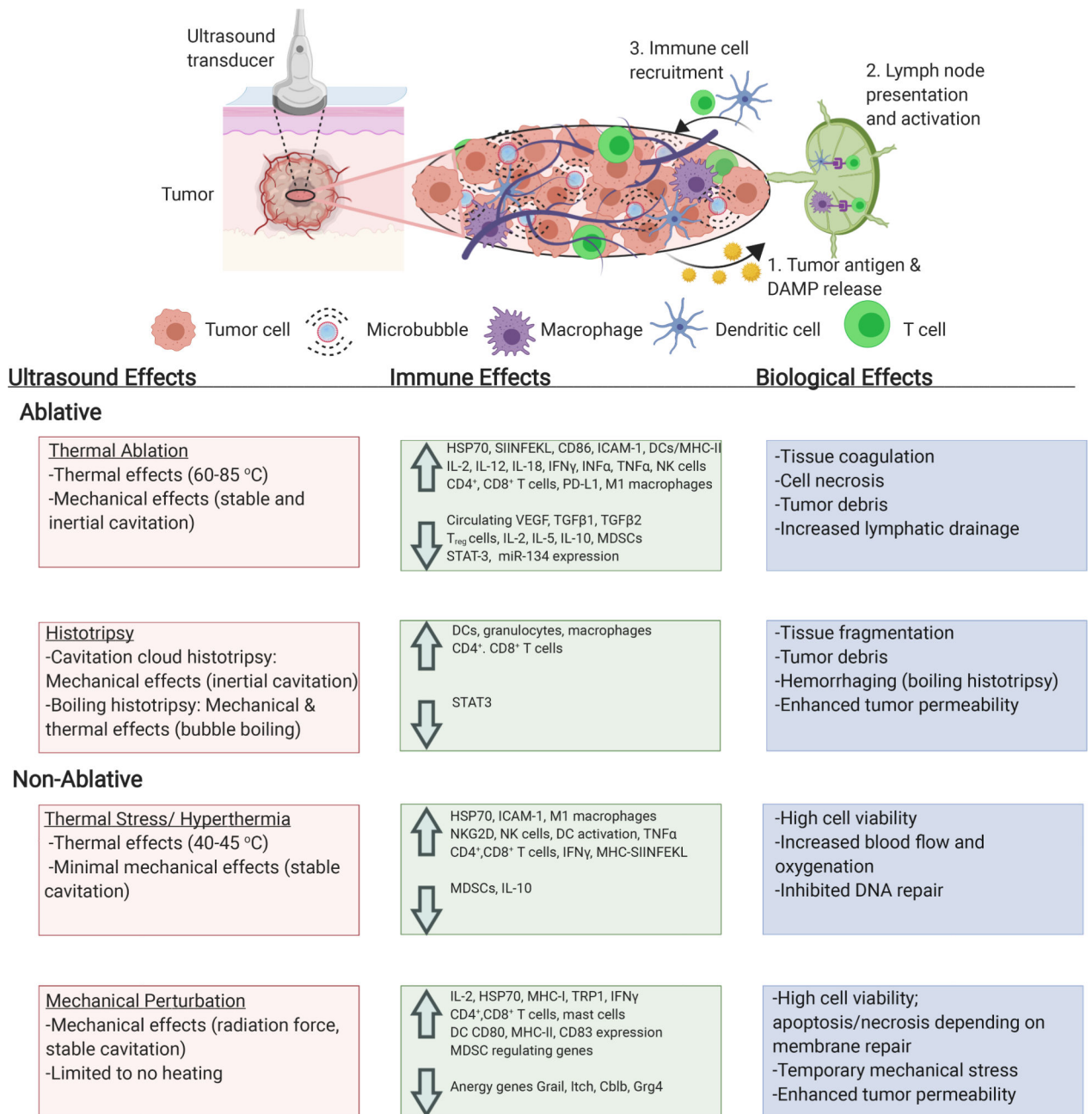


Figure 1. Biological and immune effects of ultrasound-induced thermal ablation, hyperthermia, mechanical perturbation, and histotripsy (25). Created with help of [Biorender.com](https://www.biorender.com)

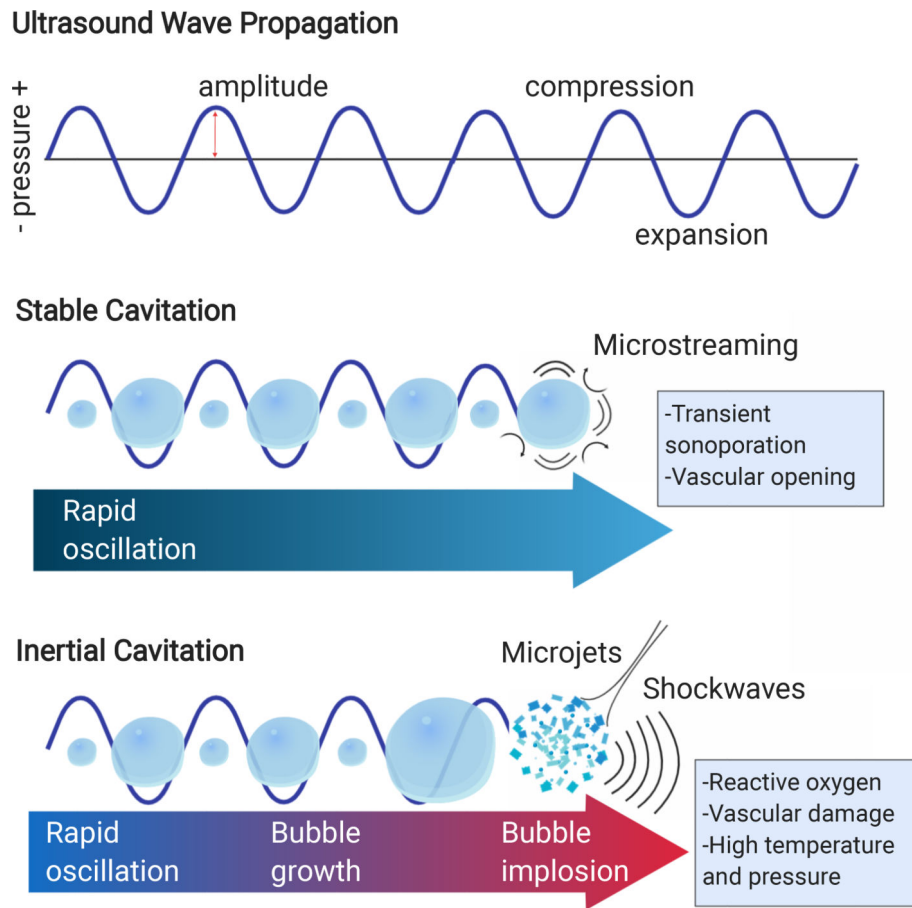


Figure 2. Microbubbles oscillate rapidly and undergo stable or inertial cavitation in response to ultrasound. Created with help of [Biorender.com](https://www.biorender.com)

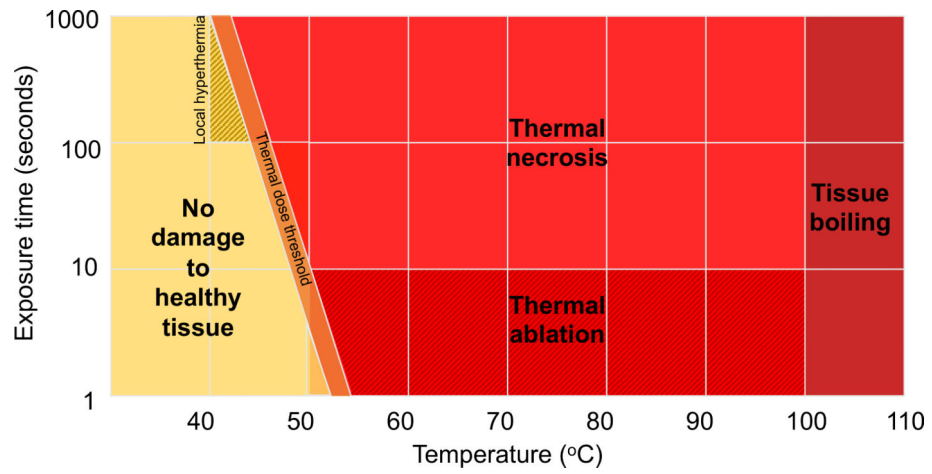


Figure 3. Tissue bioeffects of thermal ultrasound as defined by temperature and exposure time. Adapted from (157).

Range of ultrasound parameters used pre-clinically and clinically to induce thermal ablation, thermal stress, hyperthermia, mechanical perturbation and histotripsy.

Table 1.

Parameter	Thermal Ablation (28–31)	Thermal Stress/Hyperthermia (32–33)	Mechanical Perturbation (34–35)	Histotripsy (34, 36)
Frequency	200 kHz-20MHz	200 kHz-3MHz	200 kHz-3MHz	200 kHz-3MHz
Pressure	3-70 MPa	0.1–4 MPa	0.1-4 MPa	10-80 MPa
Duty Cycle	0.5-100%	0.5-100%	0.5-50%	0.01-4%
Treatment Time (per focal spot)	Seconds to minutes	Seconds to minutes/30-90 minutes	Seconds to minutes	Seconds to minutes

Table 2.

Immune and Therapeutic Effects of Focused Ultrasound Tumor Thermal Ablation

Disease	Model	Treatment & FUS Parameters	Immunologic Effect	Therapeutic Effect
Melanoma	B16F10 (C57BL/6 mouse)	-Pressure: 5.42 MPa -Power: 12.5W, 4 s at each spot, Duty cycle: 75% -Separate study combined one 10-Gray (Gy) radiation dose post-HIFU treatment	-Increase in CD45 ⁺ cells, but no increase in T cells, signifying influx of other inflammatory cells in response to tissue damage	-Loss of primary tumor and tumor-bearing limb due to HIFU. Secondary tumors necessitated sacrifice of mice. (92)
Metastatic mammary carcinoma	NDL (FVB/n mouse)	-Ablation only or ablation + immunotherapy (αPD-1 and CpG every 3-4 days for 3 doses, followed by ablation and αPD-1 or CpG every 3-7 days for 4 doses) -Pressure: 3.1 MPa, Power: 5 W, Scan Speed: 1 rps (revolutions per second), CEM43 (cumulative equivalent minutes): >5000 for a temperature of >65°C	-Ablation only increased IFN-γ-producing CD4 ⁺ T cells and CD8 ⁺ T cells, decreased T _{reg} cells. Lymphatic drainage was increased. -Immunotherapeutic priming reduced macrophages and MDSCs and increased number of IFN-γ-producing CD8 ⁺ T cells, M1 macrophage fractions, and PD-L1 expression on CD45 ⁺ producing CD8 ⁺ T cells.	-Immunotherapy primed with ablation caused 80% of mice with 1 tumor to completely respond by day 90. -60% of mice with 3 tumors completely responded compared to 25% with immunotherapy only. (59)
Melanoma, mammary adenocarcinoma & breast cancer	B16F10 (C57BL/6 mouse), NDL (FVB/n mouse) & MMTV-PyMT (transgenic mouse)	-B16F10 groups: ablation only and ablation + immunotherapy (CpG dose 4, 3, 2 and 0 days before ablation; anti-PD-1 dose 4 and 2 days before ablation) -NDL group: ablation + immunotherapy (AI) (CpG dose 10, 7, 3, and 0 days before ablation; αPD-1 dose 10 and 3 days before ablation and 4 days after ablation) -MMTV-PyMT group: ablation + immunotherapy (CpG dose 10, 7, 3, and 0 days before ablation; αPD-1 dose 10 and 3 days before ablation and 4 days after ablation) -Power: 5 and 10 W, Scan speed: 1 rps, CEM43: >5000 for a temperature of >65°C	-B16F10: Ablation only enhanced tumor fraction of immune cell expression of ovalbumin SIINFEKL peptide and number of infiltrating macrophages after 48 hours. AI-treatment induced type I IFN release and recruited CD1169 ⁺ macrophages and dendritic cells in the tumor. -NDL: AI-treatment significantly increased CD3 ⁺ , CD4 ⁺ , CD8 ⁺ T-cells in contralateral tumors compared to all groups 1 week after treatment. AI increased number of unique CDR3 rearrangements and T-cell receptor overlap between tumors and blood. -MMTV-PyMT: AI-treatment significantly increased CD8 ⁺ T-cells in contralateral tumors compared to all groups 1 week after treatment.	-B16F10: Tumor volume 4 days after treatment was reduced by AI treatment in 4 of 5 mice. -NDL: AI tumor growth reduction greater than immunotherapy alone 1 week after treatment. 100% of AI-treated and 90% of AI-contralateral tumors reduced by 1 standard deviation compared to no treatment. -MMTV-PyMT: AI tumor growth reduction greater than immunotherapy alone. (60)
Melanoma	B16F10 (C57BL/6J mouse)	-Frequency: 9.3 MHz, Power: 4.5 W, 10 s at each spot, total exposure time 120 s	-HIFU suppressed miR-134 expression and activated co-stimulatory molecules CD86 and ICAM-1 expression in the tumor. -IFN-γ and TNF-α increased in the blood.	-HIFU decreased circulating B16F10 cells and pulmonary metastasis nodules -Tumor volume at day 31 was 2/3 less using HIFU compared to sham. (95)
Hepatocellular carcinoma	H22, (C57BL/6 mouse)	-Frequency: 9.5 MHz, Power: 5 W, focal length: 8 mm, total exposure time: 220 s	-HIFU increased CD3 ⁺ and CD4 ⁺ levels in peripheral blood, increased CD4 ⁺ /CD8 ⁺ ratio, and decreased CD8 ⁺ ratio compared to sham. TNF-α and IFN-γ secretion from splenic T cells was higher in HIFU than sham and control.	-Adoptive transfer of T-cells from HIFU-treated tumors into mice with H22 tumors prolonged the 60-day survival period. (96)

Table 3.
Immune and Therapeutic Effects of Focused Ultrasound Induced Hyperthermia and Thermal Stress

Disease	Model	Treatment & FUS Parameters	Immunologic Effect	Therapeutic Effect
Colon cancer	C26, (Balb/c mouse)	-Frequency: 1 MHz, Varied intensities: 1, 2, 3, 4 W/cm ² , Varied pressures: 0.109, 0.154, 0.188, 0.217 MPa, MIs: 0.147, 0.207, 0.254, 0.283, Temperatures: 32-44°C. Duty cycle: 50%, Burst rate: 2 Hz, Treatment time: 2 min (thermal stress). -Bolus injection of decafluorobutane (DFB) bubble liposomes at 0.1 mg/mL, 30 L/mouse	-Mice with tumors were injected either with anti-CD8 ⁺ , anti-CD4 ⁺ or anti-NK cell antibody for in-vivo depletion study. -16 days after tumor inoculation, tumors that were treated and CD4 ⁺ /CD8 ⁺ depleted, CD8 ⁺ depleted or not were all significantly larger than tumors that were treated but not depleted.	-Tumoral necrosis evident at 3 and 4 W/cm ² with bubble liposome treatment -Significant tumor volume % decrease for mice treated with 3 and 4 W/cm ² and bubble liposomes. (118)
Colon cancer	C26, (Balb/c mouse)	-Hyperthermia treatment 24 hr after injection of thermosensitive liposome-laden <i>Salmonella</i> (groups: HIFU only, <i>Salmonella</i> only, <i>Salmonella</i> + HIFU, TB, TB +HIFU) -Pulse repetition frequency (PRF): 5 Hz, Power: 6 W, Duty cycle: 35%, Temp. 40-42.5°C, each point heated 60 s, total treatment time: 30 min.	-TB+HIFU group caused highest increase of M1 macrophages compared to other groups (without increase in M2), <i>Salmonella</i> and TB increased IFN- expressing CD4 ⁺ /CD8 ⁺ cells with and without HIFU, no change in MDSCs in any groups. -Significantly increased cytokine levels of TNF- α (TB+HIFU) and IL-1 (TB and <i>Salmonella</i>) and decrease in IL-10 (TB+HIFU and <i>Salmonella</i> + HIFU) compared to other groups.	-Significant tumor regression with TB+HIFU group over 5 days compared to all groups. -HIFU increased apoptotic cells. (123)
Melanoma, mammary adenocarcinoma	B16F10/B16-OVA (C57BL/6 mouse), ND/L (FVB/n mouse) & MMTV-PyMT (transgenic mouse)	-B16F10/B16OVA group: IV treatment of 6 mg/kg temperature-sensitive liposomes with doxorubicin and copper (CuDox-TSL) and B16-OVA heating to 42°C. -NDL group: IV treatment of CuDox-TSL, immunotherapy (IT) treatment of CpG (100 g) and tumor heating to 42°C, 3 days later, treatment of aPD-1 (200 g, i.p.). Another group repeated this treatment 4 days after. A third group used a treatment schedule of priming with CpG and aPD-1 on day 0, 3 and 7 followed by CuDox-TSL and heating to 42°C on day 10, followed by CpG and aPD-1 on day 15. -MMTV-PyMT group: Same treatment as NDL group with repeated treatment. -Pressure: 2.5 MPa, PRF: 100 Hz, burst duration: 0-7 ms controlled to maintain temperature at 42°C for 25 minutes.	-B16F10/B16OVA group: Distant B16F10 tumors experienced a significant increase in leukocytes, DCs and macrophages displaying the MHC-I-SIINFEKL complex compared to nontreated control. -NDL group: Treatment with CuDox-TSL and immunotherapy increased intratumoral CD8 ⁺ T cells and macrophages in both treated and distant tumors compared to nontreated control, however, CD8 ⁺ secretion of IFN-g did not increase. Tumors treated with immunotherapy only demonstrated significant increase of IFN-g secreting CD8 ⁺ cells. Foxp3 was not affected. Repeated dosing of CuDox-TSL and immunotherapy had decreased amount of CD8 ⁺ cells, IFN-g secreting CD8 ⁺ cells and MDSCs compared to one treatment. The third group of immunotherapy priming and single CuDox-TSL dose with 42°C ultrasound significantly enhanced CD8 ⁺ tumor infiltration. Repeated treatment of CuDox-TSL and ultrasound increased blood NK cells. - MMTV-PyMT group: repeated IT and CuDox-TSL with 42°C ultrasound dosing demonstrated extensive necrosis and enhanced CD8 ⁺ and macrophage infiltration compared to immunotherapy only.	-NDL group: 9 of 10 mice treated with IT priming, single CuDox-TSL dose and 42°C ultrasound experienced significant tumor and distant tumor regression at day 38. IT and dox mouse survival was 90% while IT only survival was 78% (101 days). (61)

Table 4.
Immune and Therapeutic Effects of Focused Ultrasound Mechanical Tumor Perturbation

Disease	Model	Treatment & FUS Parameters	Immunologic Effect	Therapeutic Effect
Colon cell carcinoma	CT26, mouse	<ul style="list-style-type: none"> • Pressure: 0.6 or 1.4-MPa, Power: 5 or 30W, Burst length: 100 ms, PRF: 1 Hz, Duration: 20 s each for total treatment time of 180-240 seconds • 0.1 mL/kg bolus SonoVue MBs given 10 s prior to LOFU 	<p>1.4 MPa + MB: Significant and continual increase of intratumoral CD8+ cells 1, 3 and 18 days after treatment. CD4⁺Foxp3⁺ T cells and mast cells significantly increased 1 day after treatment but subsided after 3 days.</p> <p>0.6 MPa + MB: Only significant decrease of mast cells 18 days after treatment.</p> <p>Enhanced leakage of 60 kDa dextran into tumors</p>	<p>-1.4 MPa + MB and 0.6 MPa + MB treatment resulted in 34.4% and 18.1% tumor growth reduction respectively compared to control 16 days after treatment. Treatments in the absence of MBs were not effective. (57)</p>
Colon cell carcinoma	CT26, mouse (BALB/c)	<ul style="list-style-type: none"> • 0.1 mg/mL, 30 μL perfluoropropane MBs given immediately prior to LOFU. • Frequency: 1 MHz, Burst rate: 2.0 Hz, Duty cycle: 50%, Intensity: 1-4 W/cm², PnP: 0.109-0.217 MPa, mechanical index (MI): 0.147-0.283, 2 min total duration, 35-44 °C. 	<p>Depletion of CD8⁺ T cells (not NK or CD4⁺ T cells) significantly reduced the therapeutic response, demonstrating their key role in response.</p>	<p>-60% tumor volume decrease compared to no treatment 22 days after tumor inoculation (118)</p>
Melanoma	B16F10, mouse (C57BL/6)	<ul style="list-style-type: none"> • Pressure: 2.93 MPa (80 mm focal length)/3.81 MPa (85 mm focal length), Power: 3W, Intensity: 550 W/cm², 1.5 s at each spot, total exposure time 5 min • Separate study combined 10 Gy fractionated radiation dose (IGRT) daily for 3 days, 2-4 hours post-FUS treatment 	<p>Increase in IL-2 production by CD4⁺ from tumor draining lymph node (DLN) 36 hr after LOFU. Decrease in CD4⁺ DLN expression of energy genes <i>Grail</i>, <i>Itch</i>, <i>Cblb</i> and <i>Grg4</i>. Lysates from LOFU treated tumors co-cultured with splenic dendritic cells and responder naive CD4⁺T cells activated OT-II responder T cells. These same lysates induced a significant increase of dendritic cell CD80, MHC-II and CD85 expression. Activation of T_H1-CD4⁺ T cells when LOFU-treated DLN lysates co-cultured with T cell-depleted DLN cells. No difference in tumor levels of CD11b⁺CD11c⁺ DCs or CD11b⁺Gr1⁺ MDSCs. LOFU increased expression of Hsp70, MHC-I, and TRP1.</p>	<p>-LOFU+IGRT treatment significantly delayed tumor growth 6-weeks following treatment compared to IGRT and LOFU alone. Mice treated with LOFU+IGRT experienced tumor regression from baseline and complete tumor-free response in 4 out of 5 mice (92)</p>
Colon cell carcinoma	CT26, mouse (BALB/c)	<ul style="list-style-type: none"> • aPD-1 given 30 min prior to LOFU. • 9.6 \times 10⁸ octafluoropropane MBs/kg bolus given 10 s prior to LOFU. • PnP: 1.65 MPa, 30 ms each spot, 2 min total duration 	<p>Increase in tumoral IFNγ expression at day 3. Decrease in % T_H17 cells, increase in % T_{reg} cells at day 7. No evidence of T-cell dependent treatment enhancement.</p>	<p>-USMB+aPD-1 tumors significantly smaller than all other treatment groups. One mouse (of n=6) experienced complete tumor regression after rechallenge (62)</p>